Discussion

To date, there have been many reports concerning the pathogenicity of rickettsiae (Andersson *et al.*, 1998; Li & Walker, 1998; Ogata *et al.*, 2001; Uchiyama, 2003; Joshi *et al.*, 2004; Sahni *et al.*, 2005; Whitworth *et al.*, 2005; Uchiyama *et al.*, 2006; Chan *et al.*, 2009; Fournier *et al.*, 2009; Clark *et al.*, 2011). However, the molecular basis for the pathogenesis of SFG rickettsiosis is yet to be precisely established.

To clarify the difference between the growth of pathogenic SFGR and nonpathogenic SFGR, we compared the growth kinetics of the pathogenic species *R. japonica* with those of the nonpathogenic species *R. montanensis* in mammalian cells. As expected, the growth of *R. montanensis* was restricted but that of *R. japonica* was not (Fig. 1a,b). We then examined the influence of autophagy on the growth of rickettsiae. As shown in Fig. 2, autophagy occurred in the cells that had been infected with *R. montanensis*, but was much rarer in those infected with *R. japonica* (data not shown). Thus, it is reasonable to hypothesize that pathogenic rickettsiae secrete factor(s) that restrict autophagy whereas nonpathogenic rickettsiae do not. When the *R. montanensis*-infected cells were co-infected with *R. japonica*, the growth of *R. montanensis* was rescued and was accompanied by *R. japonica* growth, as shown in Fig. 1a and b. We also found that when the order of infection was reversed in the co-infection experiment, both rickettsiae grew well (Fig. 1c,d). Moreover, we found that compared with that seen in the cells subjected to *R. montanensis* infection alone, the expression of the autophagy-related protein LC3B was restricted after the co-infection of *R. montanensis*-infected cells with *R. japonica* (Fig. 2). Single infection with *R. japonica* and the co-infection of *R. japonica*-infected cells with *R. montanensis* also resulted in autophagy restriction. Our transmission electron microscopy findings supported the results shown in Fig. 2 and indicated that rickettsiae were being digested in the autophagosome-like vacuoles of the cells that had been singly infected with *R. montanensis* but grew well in the co-infected cells (Fig. 3). These results are consistent with the hypothesis presented previously. Thus, it is suggested that the growth restriction of the nonpathogenic species *R. montanensis* is at least partly due to the autophagy that occurs in the infected cells and that the pathogenic species *R. japonica* secretes an autophagy-restriction factor(s). This factor(s) is yet to be identified.

Acknowledgements

This study was supported, in part, by a Grant-in-Aid for Scientific Research (C) (21590481) from the Japan Society for the Promotion of Science and by a Grant-in-Aid for Research on Emerging and Re-Emerging Infectious Diseases (H21-Shinkou-Ippan-006) from the Ministry of Health, Labor, and Welfare of Japan.

References

Andersson SGE, Zomorodipour A, Andersson JO *et al.* (1998) The genome sequence of *Rickettsia prowazekii* and the origin of mitochondria. *Nature* **396**: 133–140.

Bell EJ, Kohls GM, Stenner HG & Lackman DB (1963) Nonpathogenic rickettsias related to the spotted fever group isolated from ticks, *Dermacentor variabilis* and *Derrnacentor andersoni* from Eastern Montana. *J Immunol* **90**: 770–781.

Chan YGY, Cardwell MM, Hermanas TM, Uchiyama T & Martinez JJ (2009) Rickettsial outer-membrane protein B (rOmpB) mediates bacterial invasion through Ku70 in an actin, c-Cbl, clathrin and caveolin 2-dependent manner. *Cell Microbiol* **11**: 629–644.

Christie PJ (1997) *Agrobacterium tumefaciens* T-complex transport apparatus: a paradigm for a new family of multifunctional transporters in eubacteria. *J Bacteriol* **179**: 3085–3094.

Clark TR, Ellison DW, Kleba B & Hackstadt T (2011) Complementation of *Rickettsia rickettsii* relA/spoT restores a nonlytic plaque phenotype. *Infect Immun* **79**: 1631–1637.

Cullinane M, Gong L, Li X, Lazar-Adler N, Tra T, Wolvetang E, Prescott M, Boyce JD, Devenish RJ & Adler B (2008) Stimulation of autophagy suppresses the intracellular survival of *Burkholderia pseudomallei* in mammalian cell lines. *Autophagy* **4**: 744–753.

Fournier P-E, El Karkouri K, Leroy1 Q, Robert C, Giumelli B, Renesto P, Socolovschi C, Parola P, Audic S & Raoult D (2009) Analysis of the *Rickettsia africae* genome reveals that virulence acquisition in *Rickettsia* species may be explained by genome reduction. *BMC Genomics* **10**: 166.

Joshi SG, Francis CW, Silverman DJ & Sahni SK (2004) NF-κB activation suppresses host cell apoptosis during Rickettsia rickettsii infection via regulatory effects on intracellular localization or levels of apoptogenic and anti-apoptotic proteins. *FEMS Microbiol Lett* **234**: 333–341.

Li H & Walker DH (1998) rOmp A is a critical protein for the adhesion of *Rickettsia rickettsii* to host cells. *Microb Pathog* **24**: 289–298.

Lin WS, Cunneen T & Lee CY (1994) Sequence analysis and molecular characterization of genes required for the biosynthesis of type I capsular polysaccharide in *Staphylococcus aureus*. *J Bacteriol* **176**: 7005–7016.

Ogata H, Audic S, Renesto-Audiffren P *et al.* (2001) Mechanisms of evolution in *Rickettsia conorii* and *R. prowazekii*. *Science* **293**: 2093–2098.

Ogawa M, Yoshimori T, Suzuki T, Sagara H, Mizushima N & Sasakawa C (2005) Escape of intracellular *Shigella* from autophagy. *Science* **307**: 727–731.

Rydkina E, Sahni SK, Santucci LA *et al.* (2004) Selective modulation of antioxidant enzyme activities in host tissues during *Rickettsia conorii* infection. *Microb Pathog* **36**: 293–301.

Sahni SK, Rydkina E, Sahni A, Joshi SG & Silverman DJ (2005) Potential roles for regulatory oxygenases in rickettsial pathogenesis. *Ann NY Acad Sci* **1063**: 207–214.

Sasakawa C (2010) A new paradigm of bacteria-gut interplay brought through the study of *Shigella*. *Proc Jpn Acad Ser B Phys Biol Sci* **86**: 229–243.

Uchida T, Uchiyama T & Koyama AH (1988) Isolation of spotted fever group rickettsiae from humans in Japan. *J Infect Dis* **158**: 664–665.

Uchida T, Yu XJ, Uchiyama T & Walker DH (1989) Identification of a unique spotted fever group rickettsia from humans in Japan. *J Infect Dis* **159**: 1122–1126.

Uchida T, Uchiyama T, Kumano K & Walker DH (1992) *Rickettsia japonica* sp, nov, the etiological agent of spotted fever group rickettsiosis in Japan. *Int J Syst Bacteriol* **42**: 303–305.

Uchiyama T (1999) Phenotypic and genotypic homogeneity of the strains of *Rickettsia japonica* isolated from patients with Oriental spotted fever. *Microbiol Immunol* **43**: 717–721.

Uchiyama T (2003) Adherence to and invasion of Vero cells by recombinant *Escherichia coli* expressing the outer membrane protein rOmpB of *Rickettsia japonica*. *Ann NY Acad Sci* **990**: 585–590.

Uchiyama T & Uchida T (1988) Ultrastructural study on Japanese isolates of spotted fever group rickettsiae. *Microbiol Immunol* **32**: 1163–1166.

Uchiyama T, Kawano H & Kusuhara Y (2006) The major outer membrane protein rOmpB of spotted fever group rickettsiae functions in the rickettsial adherence to and invasion of Vero cells. *Microbes Infect* **8**: 801–809.

Whitworth T, Popov VL, Yu XJ, Walker DH & Bouyer DH (2005) Expression of the *Rickettsia prowazekii pld* or *tlyC* gene in *Salmonella enterica* serovar Typhimurium mediates phagosomal escape. *Infect Immun* **73**: 6668–6673.

Yoshikawa Y, Ogawa M, Hain T *et al.* (2009) *Lystera monocytogenes* ActA-mediated escape from autophagic recognision. *Nat Cell Biol* **11**: 1233–1240.

10.1111/j.1469-0691.2008.02263.x

Restriction of the growth of typhus group rickettsiae in tick cells

T. Uchiyama[1], M. Ogawa[2], M. Kishi[1], T. Yamashita[1], T. Kishimoto[2] and I. Kurane[2]

[1]Department of Virology, Institute of Health Biosciences, The University of Tokushima Graduate School, Tokushima and [2]Department of Virology 1, National Institute of Infectious Diseases, Tokyo, Japan

The vectors of typhus group rickettsiae (TGR) are lice and fleas that belong to *Insecta*. Those of spotted fever group rickettsiae (SFGR), however, are ticks classified as *Arachnida*. Until recently, the host dependency of the growth of TGR and SFGR in cells derived from arthropods had not been well documented. As for insect cells, it was reported by Rovery *et al.* that the transcription of *spoT* gene paralogues was suppressed during the infection of *Rickettsia conorii* in *Aedes albopictus* (C6/36) cells at 10°C for 38 days. Shifting the temperature to 37°C was followed by a rapid upregulation of *spoT1* gene expression [1]. Uchiyama reported that some SFGR (*Rickettsia japonica* and *Rickettsia montanensis*) do not grow in the AeAl2 cell line from *A. albopictus*, even though the rickettsiae achieved adherence and invasion [2]. On the contrary, Sakamoto *et al.* demonstrated that some non-pathogenic SFGR, *R. montanensis* and *Rickettsia peacockii* successfully grew in two mosquito cell lines (*A. albopictus* cell line Aa23 and *Anopheles gambie* cell line Sua5B) [3]. Concerning tick cell lines, several reports regarding the growth of SFGR in the cells have been published [4,5]. In this study, the growth of TGR in tick cells was examined.

The DALBE3 cell line from *Dermacentor albipictus* (a generous gift of U.G. Munderloh) and the ISE6 cell line from *Ixodes scapuralis* (generously donated by I. Takashima under agreement of U.G. Munderloh) were used as tick cells. As mammalian cells, Vero and ECV304 cells were used. These cells were inoculated with *R. japonica*, strain YH and *R. conorii*, strain Malish 7 as SFGR and *Rickettsia prowazekii*, strain Breinl and *Rickettsia typhi*, strain Wilmington as TGR at a multiplicity of infection (MOI) of 0.1 PFU/cell. The infected cells were cultured at 34°C in a medium described previously [4,5]. The medium was changed every 3 days and the yields of rickettsiae were plaque-assayed on Vero cell monolayers. As shown in Fig. 1(a), SFGR grew well in DALBE3 and ISE6 cells as well as in Vero and ECV304 cells (data from ISE6, Vero and ECV304 cells are not shown). However, growth of TGR was restricted in these tick cells contrary to their growth in Vero and ECV304 mammalian cells (data from ISE6, Vero and ECV304 cells are not shown). Rickettsial infectivity decreased to an undetectable level up to 2 weeks after infection.

Because the growth of TGR in these cells was restricted, the adherence step was analysed to determine if it was completed. We inoculated the tick cells with rickettsiae at an MOI of 1.0 PFU/cell and incubated these cells for 5, 10, 60 or 180 min at 25°C. As shown in Fig. 1b, the adherence of these cells by TGR was successfully completed as were those in other combinations of rickettsiae and host cells, although the extent of adherence differed among the combinations tested. We also performed Giménez staining of the tick cells inoculated with either group of rickettsiae at an MOI of 50 PFU/mL and found that the cells showed adherence and/or invasion by rickettsiae (data not shown).

Transmission electron microscopy was performed to confirm these findings and examine morphological changes. DALBE3 cells were inoculated with TGR and SFGR at an MOI of 50 PFU/cell and incubated at 25°C for 10 min, 60 min, and 180 min, and then cultured at 34°C for 24 h and 72 h until fixed. Thin sections of the samples were observed under a Hitachi H-7650 transmission electron microscope. DALBE3 cells demonstrated adherence and invasion by these rickettsiae independent of their group (data not shown). Rickettsiae under the process of escaping from phagosomes to the cytoplasm after being engulfed by DALBE3 cells were also shown. Thus, it is suggested that restriction occurred after these steps. Further analyses of the restrictive steps

Corresponding author and reprint requests: T. Uchiyama, Department of Virology, Institute of Health Biosciences, The University of Tokushima Graduate School, 3-18-15 Kuramoto, Tokushima 770–8503, Japan
E-mail: uchiyama@basic.med.tokushima-u.ac.jp

No conflicts of interest declared.

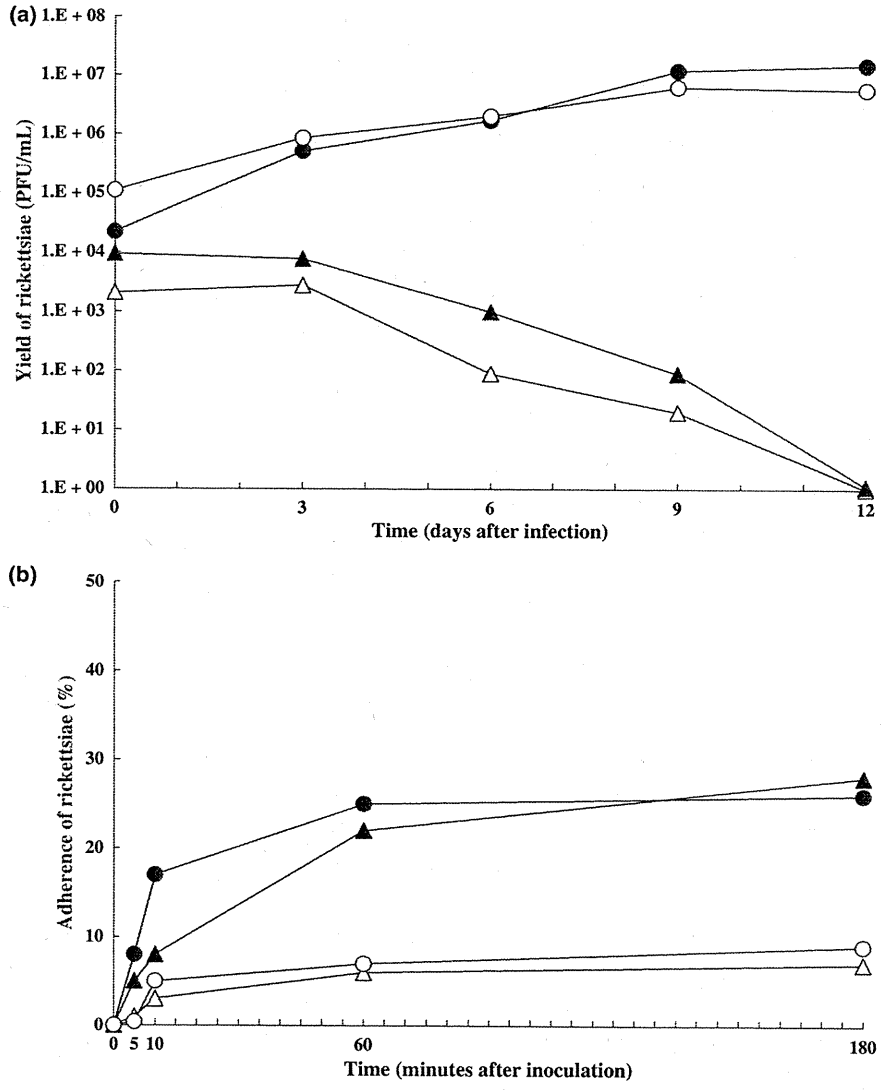

Fig. 1. (a) Growth of SFGR and TGR in DALBE3 cells. (b) Adherence of DALBE3 cells by SFGR and TGR. *R. japonica* (closed circle), *R. conorii* (open circle), *R. prowazekii* (closed triangle), and *R. typhi* (open triangle).

after invasion of TGR into DALBE3 cells are in progress.

ACKNOWLEDGEMENTS

This study was partially supported by Grant-in-Aid for Scientific Research C 19590448 from the Japan Society for the Promotion of Science (to TU).

REFERENCES

1. Rovery C, Renesto P, Crapoulet N *et al.* Transcription response of *Rickettsia conorii* exposed to temperature variation and stress starvation. *Res Microbiol* 2005; **156:** 211–218.
2. Uchiyama T. Growth of typhus group and spotted fever group rickettsiae in insect cells. *Ann N Y Acad Sci* 2005; **1063:** 215–221.
3. Sakamoto JM, Azad AF. Propagation of arthropod-borne *Rickettsia* spp. in two mosquito cell lines. *Appl Environ Microbiol* 2007; **73:** 6637–6643.
4. Policastro PF, Munderloh UG, Fischer ER, Hackstadt T. *Rickettsia rickettsii* growth and temperature-inducible protein expression in embryonic tick cell lines. *J Med Microbiol* 1997; **46:** 839–845.
5. Munderloh UG, Hayes SF, Cummings J, Kurtti TJ. Microscopy of spotted fever rickettsia movement through tick cells. *Microsc Microanal* 1998; **4:** 115–121.

10.1111/j.1469-0691.2008.02157.x

Shotgun proteomics of *Orientia tsutsugamushi*

M. Ogawa[1], F. Shinkai-Ouchi[2], M. Matsutani[3], T. Uchiyama[4], K. Hagiwara[2], K. Hanada[2], I. Kurane[1] and T. Kishimoto[1]

[1]Department of Virology 1, [2]Department of Biochemistry and Cell Biology, National Institute of Infectious Diseases, Toyama, Shinjuku-ku, Tokyo, [3]Department of Microbiology and Immunology, Yamaguchi University School of Medicine, Ube, Yamaguchi and [4]Department of Virology, Institute of Health Biosciences, The University of Tokushima Graduate School, Tokushima-shi, Tokushima, Japan

Orientia tsutsugamushi is one of the obligate intracellular bacteria, and causes Tsutsugamushi disease (scrub typhus). The whole genome sequence of Boryong strain revealed some characteristics of this bacterium, such as a type IV secretion system, many histidine kinases, SpoT, Tra, and ankyrin repeat- and tetratricopeptide repeat (TPR)-containing proteins [1]. Additionally, the structure of the genome of *O. tsutsugamushi* was completely different from those of other rickettsia that have been previously reported. We performed a combination assay of SDS-PAGE and LC-MSMS (GeLC-MSMS) to identify expressed proteins and study the protein profile of this bacterium.

The Kuroki strain of *O. tsutsugamsuhi*, which is very close to the Boryong strain, was propagated in L929 cells and purified by the Renografin density method. About 50 μg of the purified rickettsia was subjected to SDS-PAGE, and the gel was cut into about 40 pieces. Then, the pieces of gel were subjected to in-gel digestion with trypsin or endoproteinase Lys-C. Trypsin digests proteins at the arginine and lysine sites, whereas Lys-C digests only at the lysine site. Finally, the digested peptides were subjected to LC-MSMS analysis (Magic2002 Michrom Biosource Inc., Auburn, CA, USA and LCQ-DECAXP Thermo Fisher Scientific, San Jose, CA, USA). Two different procedures were used, involving different sizes of column (InertsilODS3; GL Science Inc., Shinjuku, Tokyo, Japan) and acetonitrile concentration gradient times: a 0.1 mm × 5 cm column and a 60-min gradient time; and a 0.1 mm × 15 cm column and a 120-min gradient time. For data analysis, proteins were identified using the TurboSequest algorithm in the Bioworks 3.1 package software (Thermo fisher Scientific) and the *O. tsutsugamushi* database (NCBI, National Center for Biotechnology Information, Bethesda, MD, USA). The criteria for positive identification of peptides were cross-correlation number (X_{corr}) >1.0 for singly charged ions, X_{corr} >1.5 for doubly charged ions, and X_{corr} >2.0 for triply charged ions. Only the best-matched peptides were considered.

The strategy using both trypsin and Lys-C for in-gel digestion and two sets of columns and gradient times for LC-MSMS had the great advantage of identifying proteins, especially proteins of lower molecular mass (<50 kDa). One hundred and sixty-five proteins were identified by both trypsin and Lys-C digestion, 68 proteins only by Lys-C, and 351 only by trypsin digestion. Finally, the strategy allowed us to identify 584 of 1152 proteins that are annotated on the genome of *O. tsutsugamsuhi* (49.4%). The identified proteins included 67.9% (127/187) of essential proteins of the potential minimum bacterium as previously proposed by Gil *et al.* [2] (Table 1). The identified proteins were classified into COG functional categories [3,4] and compared with those of other rickettsia and bacteria [5]. Comparatively, in *O. tsutsugamushi*, the category 'translation' was higher than the other categories, whereas categories of the entire metabolism were not as high as in other rickettsia and obligate intracellular

Table 1. Some characteristics of identified proteins

Characteristics	Numbers of identified proteins/ proposed or annotated proteins
Esssential proteins[a]	127/187
TPR[b]	5/17
Ankyrin repeat	22/40
SpoT	8/24
Histidine kinase	5/31
Type IV secretion system	13/15
Tra family	11/107

[a]These proteins were proposed by Gil *et al.*
[b]tetratricopeptide repeat-containing proteins.

Corresponding author and reprint requests: T. Kishimoto, Department of Virology 1, National Institute of Infectious Diseases, 1-23-1 Toyama, Shinjuku-ku, Tokyo 162-8640, Japan
E-mail: kisimoto@nih.go.jp

No conflicts of interest declared.

bacteria. This type of protein profile is common among obligate intracellular bacteria, although the genome construction of each species is different. This result may suggest similar genome evolution was undergone among different intracellular bacteria. In short, during evolution, the obligate intracellular bacteria lacked some proteins of important function, such as concerning metabolism, and depended instead on their host cells, whereas they may have conserved some other proteins, for example, the proteins categorised into function of 'translation', to survive in the host cells. The identified proteins include five of 17 TPR-containing and 22 of 40 ankyrin repeat-containing proteins, which are exogenous and of mammalian origin, and may play important roles in protein–protein interactions. They also include five of 31 histidine kinases, which play a role in sensor and signal transduction in response to changes in the bacterial environment, and eight of 24 SpoT family proteins, which play a role in stringent control in response to energy starvation. These proteins are suggested to play important roles in survival or adaptation to environmental change. Furthermore, they also include 13 of 15 type IV secretion system proteins and 11 of 107 Tra family proteins, which play a role in gene transfer between rickettsia or other bacteria (Table 1). The PSORTb program predicted three outer membrane proteins among unknown functional proteins and one extracellular protein that are potential immunogenic proteins. This study showed that the protein profile of *O. tsutsugamushi* is very similar to those of other obligate intracellular bacteria, and also contains some potentially virulent and immunogenic proteins. These results are useful and important for the further study of virulence, bacteria–host interactions, and also the development of new serodiagnostic tools.

REFERENCES

1. Cho NH, Kim HR, Lee JH, *et al.* The *Orientia tsutsugamushi* genome reveals massive proliferation of conjugative type IV secretion system and host-cell interaction genes. *Proc Natl Acad Sci USA* 2007; **104:** 7981–7986.
2. Gil R, Silva FJ, Pereto J, Moya A. Determination of the core of a minimal bacterial gene set. *Microbiol Mol Biol Rev* 2004; **68:** 518–537.
3. Tatusov RL, Galperin MY, Natale DA, Koonin EV. The COG database: a tool for genome-scale analysis of protein functions and evolution. *Nucleic Acids Res* 2000; **28:** 33–36.
4. Tatusov RL, Natale DA, Garkavtsev IV *et al.* The COG database: new developments in phylogenetic classification of proteins from complete genomes. *Nucleic Acids Res* 2001; **29:** 22–28.
5. Ogawa M, Renesto P, Azza S *et al.* Proteome analysis of *Rickettsia felis* highlights the expression profile of intracellular bacteria. *Proteomics* 2007; **7:** 1232–1248.

Cellular Microbiology (2009) **11**(4), 629–644

doi:10.1111/j.1462-5822.2008.01279.x
First published online 7 January 2009

Rickettsial outer-membrane protein B (rOmpB) mediates bacterial invasion through Ku70 in an actin, c-Cbl, clathrin and caveolin 2-dependent manner

Yvonne G. Y. Chan,[1] Marissa M. Cardwell,[1] Timothy M. Hermanas,[1] Tsuneo Uchiyama[2] and Juan J. Martinez[1]*

[1]*Department of Microbiology, University of Chicago, 920 East 58th Street, Cummings Life Sciences Center 707A, Chicago, IL 60637, USA.*

[2]*Department of Virology, Institute of Health Biosciences, University of Tokushima Graduate School, 3-18-15 Kuramoto-cho, Tokushima-shi, Tokushima 770-8503, Japan.*

Summary

***Rickettsia conorii*, an obligate intracellular tick-borne pathogen and the causative agent of Mediterranean spotted fever, binds to and invades non-phagocytic mammalian cells. Previous work identified Ku70 as a mammalian receptor involved in the invasion process and identified the rickettsial autotransporter protein, rOmpB, as a ligand; however, little is known about the role of Ku70–rOmpB interactions in the bacterial invasion process. Using an *Escherichia coli* heterologous expression system, we show here that rOmpB mediates attachment to mammalian cells and entry in a Ku70-dependent process. A purified recombinant peptide corresponding to the rOmpB passenger domain interacts with Ku70 and serves as a competitive inhibitor of adherence. We observe that rOmpB-mediated infection culminates in actin recruitment at the bacterial foci, and that this entry process relies in part on actin polymerization likely imparted through protein tyrosine kinase and phosphoinositide 3-kinase-dependent activities and microtubule stability. Small-interfering RNA studies targeting components of the endocytic pathway reveal that entry by rOmpB is dependent on c-Cbl, clathrin and caveolin-2. Together, these results illustrate that rOmpB is sufficient to mediate Ku70-dependent invasion of mammalian cells and that clathrin- and caveolin-dependent endocytic events likely contribute to the internalization process.**

Received 18 August, 2008; revised 11 December, 2008; accepted 15 December, 2008. *For correspondence. E-mail jmartine@bsd.uchicago.edu; Tel. (+1) 773 834 4556; Fax (+1) 773 834 8150.

Introduction

Rickettsiae are Gram-negative obligate intracellular pathogens transmitted to humans via arthropod vectors (Hackstadt, 1996). They are divided into two groups, the typhus group and the spotted fever group (SFG), based on differences in the diseases that they cause and the presence of the outer membrane proteins, rOmpA and rOmpB (Vishwanath, 1991). Members of both groups are historically responsible for severe human diseases (Hackstadt, 1996) and are Category B and C Select Agents as defined by the National Institute of Allergy and Infectious Diseases (NIAID). *Rickettsia conorii*, the causative agent of Mediterranean spotted fever, is transmitted into the vasculature of the host by tick-bite inoculation (Hackstadt, 1996). Subsequent replication in endothelial cells may lead to localized dermal and epidermal necrosis called an eschar or tache noire (Walker *et al.*, 1988). Further damage to the vascular endothelium and infiltration of perivascular mononuclear cells often causes increased fluid leakage into the interstitial space, ultimately resulting in a characteristic dermal rash and acute renal failure with peripheral oedema (Hand *et al.*, 1970; Walker *et al.*, 1988). Damage to target endothelial cells especially in the lungs and brain may result in the most severe manifestations of disease including pulmonary oedema and interstitial pneumonia. Although endothelial cells are the main target cell type for SFG rickettsia, *R. conorii* can attach to and invade different cell types *in vitro* and *in vivo* and spread via lymphatic vessels to lymph nodes or the bloodstream to various tissues including the lungs, spleen, liver, kidneys and heart (Walker and Gear, 1985). Initial clinical symptoms include those of a flu-like syndrome, often leading to misdiagnosis and inappropriate treatment. Although infections are controlled by broad-spectrum antibiotic therapy, untreated or misdiagnosed Mediterranean spotted fever is associated with severe morbidity and mortality (Yagupsky and Wolach, 1993).

Adherence to and subsequent invasion of target cells is critical for the establishment of a successful rickettsial infection. Electron micrographs of rickettsia–host cell interactions (Teysseire *et al.*, 1995; Gouin *et al.*, 1999) suggest that entry of *R. conorii* morphologically and mechanistically resembles a zipper-like invasion strategy, in which the invasion of non-phagocytic mammalian cells is mediated by the interactions between specific bacterial ligands and host receptors, leading to localized actin recruitment around the bacterium (reviewed in Cossart and Sansonetti, 2004). Previous work confirmed that host actin polymerization plays a crucial role in *R. conorii* entry and that actin dynamics during *R. conorii* entry are in part governed by the actin nucleating protein complex, Arp2/3. Various approaches used to disrupt signalling pathways that directly or indirectly activate the Arp2/3 complex revealed that *R. conorii* utilizes pathways involving Cdc42, phosphoinositide 3-kinase, c-Src and other protein tyrosine kinase activities to enter non-phagocytic cells (Martinez and Cossart, 2004).

A recent bioinformatics analysis of sequenced rickettsial genomes identified a family of genes termed *sca* (surface cell antigens) encoding putative outer membrane proteins (Blanc *et al.*, 2005). Five genes in this family, namely *sca0* (*ompA*), *sca1*, *sca2*, *sca4* and *sca5* (*ompB*) are highly conserved among the majority of SFG rickettsiae (Roux and Raoult, 2000; Blanc *et al.*, 2005). Interestingly, the predicted proteins encoded by *ompA*, *sca1*, *sca2* and *ompB* share homology with a family of proteins in Gram-negative bacteria called autotransporters, many of which are known virulence factors (Henderson and Nataro, 2001; Jacob-Dubuisson *et al.*, 2004). These proteins have modular structures composed of an N-terminal signal peptide, followed by a 'passenger domain' that carries out the specific function(s) of the protein, and then a C-terminal 'translocation module' that serves as a putative β-barrel rich pore for the secretion of the N-terminal passenger domain across the outer membrane (Jacob-Dubuisson *et al.*, 2004).

Two Sca proteins, rOmpA and rOmpB, are expressed on the surface of nearly all SFG rickettsiae (Hackstadt *et al.*, 1992) and have been shown to be important for attachment to mammalian cells *in vitro* (Li and Walker, 1998; Uchiyama *et al.*, 2006) and for eliciting protective humoral immune responses *in vivo* (Li and Walker, 1998; Diaz-Montero *et al.*, 2001; Feng *et al.*, 2004a,b). rOmpB, the more abundant of the two, is expressed as a preprotein (168 kDa) and cleaved to release a passenger domain (120 kDa) from the β-barrel translocation domain (32 kDa), leaving the mature 120 kDa domain associated with the outer leaflet of the outer membrane (Hackstadt *et al.*, 1992). The high degree of shared sequence identity and homology of rOmpB molecules expressed by closely related and divergent rickettsia suggest that rOmpB may also be functionally conserved (Blanc *et al.*, 2005). The full-length rOmpB from *R. japonica*, a rickettsial species closely related to *R. conorii*, is sufficient to mediate adherence and invasion of Vero cells when expressed in non-invasive *Escherichia coli* (Uchiyama *et al.*, 2006). The *R. conorii* rOmpB β-peptide has been shown to interact with mammalian surface proteins (Renesto *et al.*, 2006). Together, these studies emphasized an important role for rOmpB in rickettsial virulence.

Previous work has identified a 70 kDa protein, Ku70, from mammalian cell lines as a receptor involved in *R. conorii* entry (Martinez *et al.*, 2005). Ku70 is multifaceted in its cellular roles and compartmentalization, as it is found localized to the nucleus where it complexes with Ku80 and PARP to form the DNA–protein kinase complex for DNA non-homologous end joining; in the cytoplasm, where it sequesters Bax from the mitochondria as an inhibitor of the intrinsic apoptotic pathway; and at the plasma membrane, where as a possible heterodimer with Ku80, it has been shown to mediate cell–cell adhesion, extracellular matrix attachment through interaction with fibronectin (reviewed in Muller *et al.*, 2005), and matrix invasion by modulation of matrix metalloproteases during angiogenesis or tumour invasion (Monferran *et al.*, 2004a). Although ubiquitously expressed in mammalian cells, Ku70 is localized in abundance on the surface of a subset of cell types including non-transformed endothelial cells, as well as tumour cell lines including HeLa and Vero (Muller *et al.*, 2005). By affinity chromatography approaches, rOmpB from *R. conorii* was identified as the sole rickettsial ligand of Ku70 (Martinez *et al.*, 2005). These results suggested that rOmpB-expressing SFG rickettsia may have evolved strategies to utilize Ku70 on the surface of target cells to initiate signals leading to rickettsial uptake; however, the mechanisms through which rOmpB and Ku70 induces cellular invasion remained unknown.

In this study, we further characterize the roles of *R. conorii* rOmpB in early bacterial–host interactions. Using a heterologous *E. coli* expression system, we determined that expression of rOmpB is sufficient to mediate association with and invasion of non-phagocytic mammalian cells, and that this invasion process is Ku70-dependent. We find that purified recombinant rOmpB passenger domain interacts with Ku70 and additionally functions as a competitive inhibitor of bacterial attachment. Through the use of pharmacological inhibitors, we show that rOmpB–Ku70-mediated bacterial uptake relies in part on actin polymerization, microtubule stability and protein tyrosine kinase and phosphoinositide 3-kinase activities. We also observe that the E3 ubiquitin ligase, c-Cbl, is involved in rOmpB-mediated uptake, and that depletion of components of the endocytic machinery, namely clathrin and caveolin-2, inhibits rOmpB-mediated

invasion of HeLa cells. Our findings continue to stress the importance of rOmpB in the rickettsial entry process and provide the first insight into the signalling involved in Ku70-dependent internalization.

Results

Heterologous expression of Rickettsia *outer membrane protein B in* E. coli

To study the contribution of rOmpB and Ku70 in *R. conorii* invasion, we adapted an *E. coli*-based heterologous protein expression system for the study of rickettsial antigens (Uchiyama *et al.*, 2006). The full-length *R. conorii ompB* gene either including or excluding the endogenous rOmpB signal sequence was cloned into the *E. coli* isopropyl-β-D-thiogalactopyranoside (IPTG)-inducible expression vector, pET-22b, resulting in plasmids pJJM104 and pYC9 respectively (Fig. 1A). The plasmid, pET22-RJPOB, encodes the full-length *R. japonica* rOmpB allele and was used as a positive control (Uchiyama *et al.*, 2006). The plasmids were transformed into the *E. coli* expression strain, BL21(DE3), and the resulting strains were induced for surface protein expression. Biochemical fractionation of the induced *E. coli* strains indicates that rOmpB localizes to the outer membrane of rOmpB-expressing strains, as detected by Western immunoblotting with anti-6xHis antisera and rabbit hyper-immune sera against *R. conorii* (αRc7). To determine whether rOmpB expressed in *E. coli* is surface-exposed, IPTG-induced and uninduced *E. coli* BL21(DE3) carrying the pET22-b, pYC9 or pET22-RJPOB were fixed and processed for immunofluorescence using the αRc7 antibody. Figure 1C shows positive rOmpB staining in IPTG-induced rOmpB-expressing strains, which is absent in uninduced or empty vector strains. Negative propidium iodide staining indicates that αRc7-positive staining is not the result of membrane permeabilization, illustrating that rOmpB is indeed surface exposed in the *E. coli* heterologous expression system.

rOmpB expression in E. coli *is sufficient to mediate association to non-phagocytic human epithelial cells*

We then assayed for the ability of rOmpB-expressing *E. coli* BL21(DE3) strains to mediate attachment to mammalian cells using immunofluorescence-based and colony-forming unit-based assays, as previously described (Martinez *et al.*, 2000; Martinez and Cossart, 2004), relative to those containing the empty vector. *E. coli* BL21(DE3) (pET22-RJPOB), a strain encoding

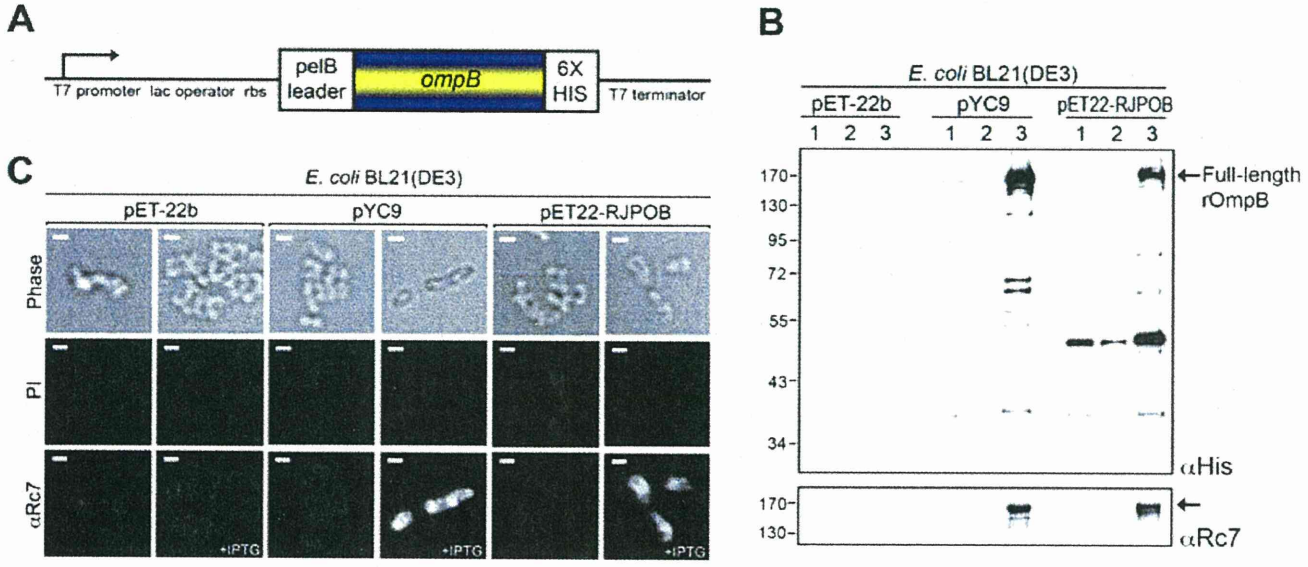

Fig. 1. Surface expression of recombinant epitope tagged rOmpB in *E. coli*.
A. Schematic of the pET-22b expression vector showing the relevant features on the 5′ and 3′ ends of the *ompB* gene. The vector encodes an N-terminal *E. coli* PelB signal sequence to direct fusion proteins through the Sec secretion pathway, as well as a C-terminal 6xHis tag.
B. Western immunoblot analysis of (1) whole cell bacterial lysate, (2) soluble and inner membrane and (3) outer membrane fractions using anti-6xHis rabbit sera (top panel) or an anti-*R. conorii* rabbit hyper-immune sera (αRc7, bottom panel). The plasmid pYC9 encodes the full-length rOmpB from *R. conorii*, while pET22-RJPOB encodes the full-length rOmpB from *R. japonica*. Arrows denote the full-length rOmpB species.
C. Immunofluorescence staining for surface-exposed rOmpB in uninduced (–IPTG) or induced (+IPTG) *E. coli* using an anti-*R. conorii* rabbit hyper-immune sera (αRc7, bottom panels). Top row panels show phase images of the *E. coli*. Propidium iodide staining (PI, middle row panels) was used to confirm that positive αRc7 staining was not a result of increased bacterial membrane permeabilization. Scale bars = 1 μm.

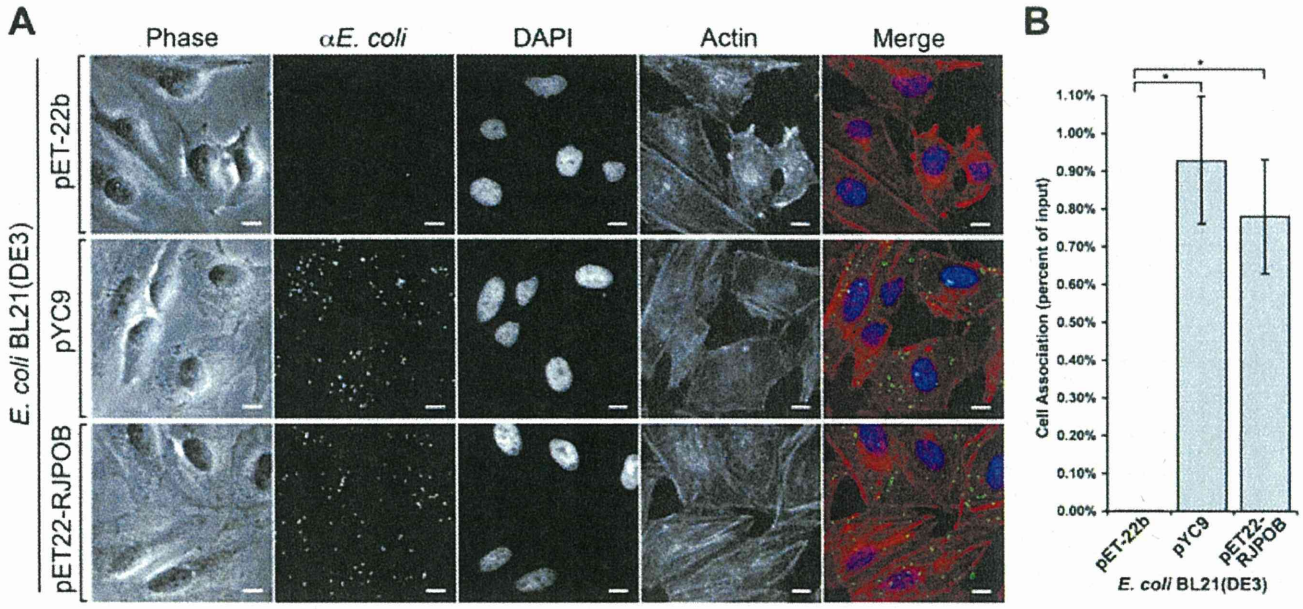

Fig. 2. Expression of rOmpB in *E. coli* sufficiently mediates association to cultured mammalian cells.
A. Fluorescence micrographs of monolayers of HeLa cells infected with *E. coli* BL21(DE3) expressing the empty vector (pET-22b) and full-length rOmpB proteins from *R. conorii* (pYC9) or *R. japonica* (pET22-RJPOB). HeLa cells seeded at 90% confluency were infected for 20 min at 37°C, then washed repeatedly with PBS and processed for immunofluorescence. Scale bars = 10 μm.
B. Colony-forming unit-based quantification of bacterial adherence on host epithelial cells. Confluent monolayers of HeLa cells were infected for 20 min at 37°C with induced cultures of *E. coli* BL21(DE3) as in A. Cell-associated bacteria were extracted from host cells by detergent lysis, and plated for colony-forming units. Association was determined as the % colony-forming units of cell-associated bacteria from the initial bacterial inoculums. *P*-values were determined by a two-tailed Student's *t*-test, $^*P < 0.05$.

rOmpB from the closely related SFG rickettsia, *R. japonica* (Uchiyama *et al.*, 2006), was utilized as a positive control in these assays. As shown in Fig. 2A, expression of either full-length rOmpB from *R. conorii*, pYC9, or *R. japonica*, pET22-RJPOB, is sufficient to mediate cell association to cultured HeLa cells compared with *E. coli* expressing the empty vector, pET-22b. Quantification of adherence using a colony-forming unit-based assay confirmed these results (Fig. 2B, see *Experimental procedures*).

rOmpB expression is sufficient to mediate E. coli *invasion of epithelial cells*

We sought to interrogate whether rOmpB expression in *E. coli* could mediate invasion of mammalian cells. HeLa cells infected for 60 min with *E. coli* expressing the *R. conorii* or *R. japonica* rOmpB allele were examined by scanning electron microscopy. Many of the cell-associated, rOmpB-expressing *E. coli* appeared entangled in microvilli (Fig. 3A, left panels), which are present in great abundance on the surface of HeLa cells. In some cases, rOmpB-expressing *E. coli*-infected HeLa cells exhibited highly suggestive membrane rearrangements implicative of bacterial internalization (Fig. 3A, arrows). In contrast, *E. coli* expressing the empty vector were scarce and difficult to find; those on the cell surface appeared passively associated and did not exhibit any sort of interaction with the microvilli (data not shown). Examination of cells infected with rOmpB-expressing *E. coli* using transmission electron microscopy showed internalized, often vacuole-enclosed bacteria (Fig. 3B), demonstrating a role for rOmpB in mediating bacterial invasion. To quantitatively assess the ability of rOmpB to stimulate bacterial internalization in mammalian cells, we utilized a gentamicin protection assay (see *Experimental procedures*). Consistent with our microscopy data, *E. coli* expression of full-length rOmpB protein in the absence of other putative rickettsial virulence factors was able to mediate invasion of non-phagocytic HeLa cells (Fig. 3C). Similar observations and results were seen in Vero cells (data not shown). The presence of the endogenous rOmpB signal sequence in conjunction with the pET-22b vector-encoded PelB signal sequence had no apparent influence on rOmpB-mediated cell association and invasion (data not shown); therefore *E. coli* BL21(DE3) (pJJM104) and *E. coli* BL21(DE3) (pYC9) were used interchangeably.

rOmpB-mediated invasion is Ku70-dependent

Previous work identified Ku70 as a receptor for *R. conorii* invasion in mammalian cells, and rOmpB as a Ku70 ligand (Martinez *et al.*, 2005). To determine whether Ku70 functions in rOmpB-mediated bacterial invasion, we per-

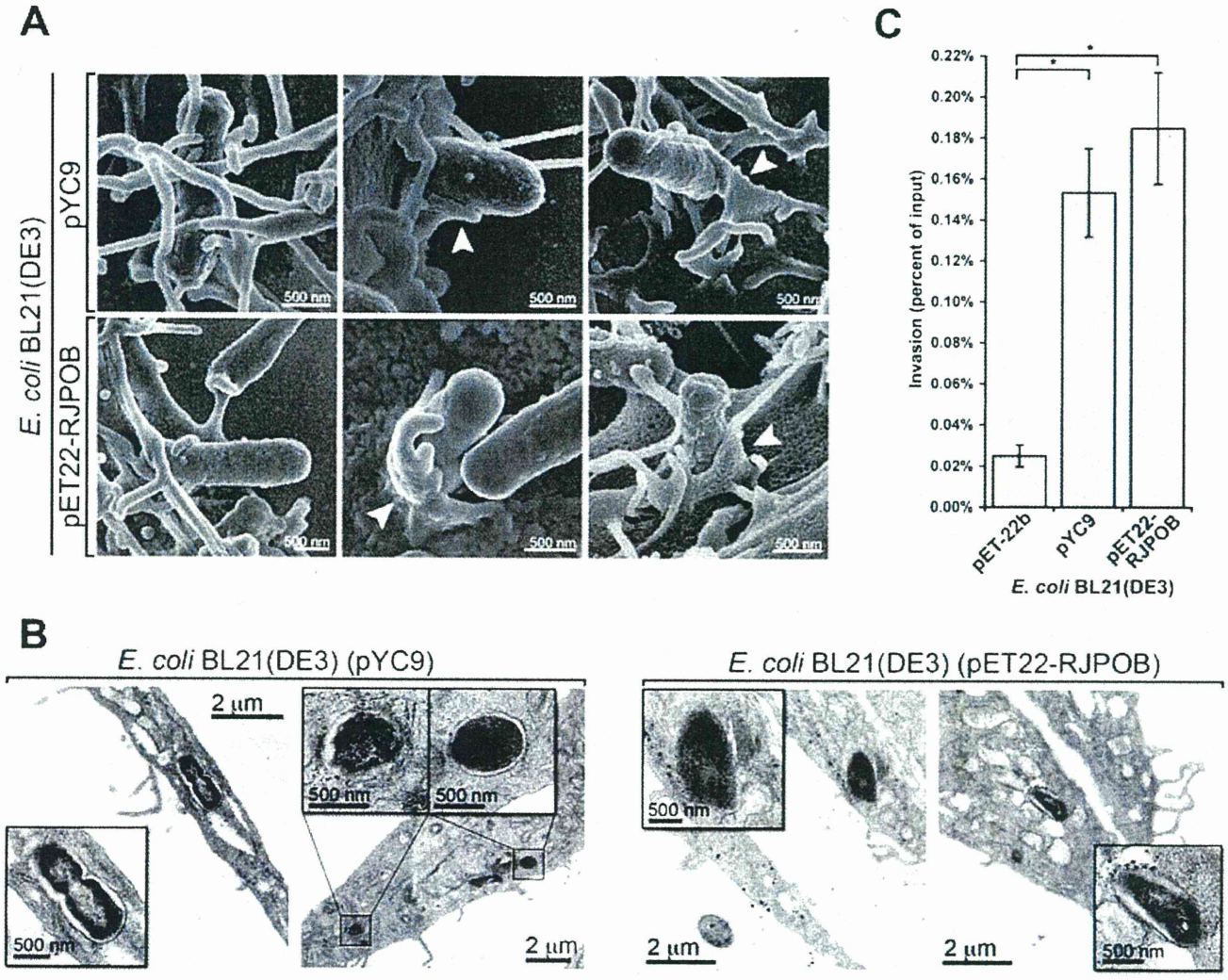

Fig. 3. rOmpB expression in *E. coli* mediates invasion of cultured mammalian cells.
A. Scanning electron microscopy (SEM) examining the surface interaction of rOmpB-expressing *E. coli* with HeLa cells. HeLa cell monolayers on glass coverslips were infected with for 1 h, and then processed for SEM. White arrowheads highlight possible rOmpB-mediated cellular membrane rearrangements. Scale bars = 500 nm.
B. Transmission electron microscopy (TEM) of internalized rOmpB-expressing *E. coli* in HeLa cells. HeLa cell monolayers were infected for 2 h with *E. coli* BL21(DE3) expressing rOmpB, then processed and visualized by TEM. Inset: enlargement of the internalized *E. coli*. Scale bars are as noted [2 µm, 0.5 µm (inset)].
C. Bacterial invasion of HeLa cells. HeLa cell monolayers were infected for 1 h with *E. coli* BL21(DE3) expressing the empty vector (pET-22b) or rOmpB (pYC9 or pET22-RJPOB) and assessed for invasion using the gentamicin protection assay. Invasion is presented as the per cent of bacteria recovered after the gentamicin challenge out of the inoculums. Actual percentages varied from assay to assay (ranging from 0.1% to 0.5%) depending on the passage number of mammalian cells used and the expression of rOmpB on the *E. coli* outer membrane. *P*-values were determined by a two-tailed Student's *t*-test, $^*P < 0.05$.

formed invasion assays on HeLa cells transfected with either a scrambled control small-interfering RNA (siRNA) or Ku70 siRNA. Reduction of endogenous Ku70 protein levels in HeLa cells did not significantly affect rOmpB-mediated cell association (Fig. 4A), in agreement with a previous study examining *R. conorii* adherence to Ku70 siRNA-treated mammalian cells (Martinez *et al.*, 2005). In contrast, invasion of rOmpB-expressing *E. coli* strains into Ku70-depleted HeLa cells decreased to levels comparable with that of the non-invasive, vector control (Fig. 4B). These results suggest that while rOmpB may interact with multiple eukaryotic plasma membrane proteins to mediate cell association, interactions via Ku70 productively mediate bacterial entry.

Recombinant rOmpB$_{36-1334}$ interacts with Ku70 and functions as a competitive inhibitor of cell association

Numerous studies (Martinez *et al.*, 2005; Uchiyama *et al.*, 2006) suggest that a functional component of the

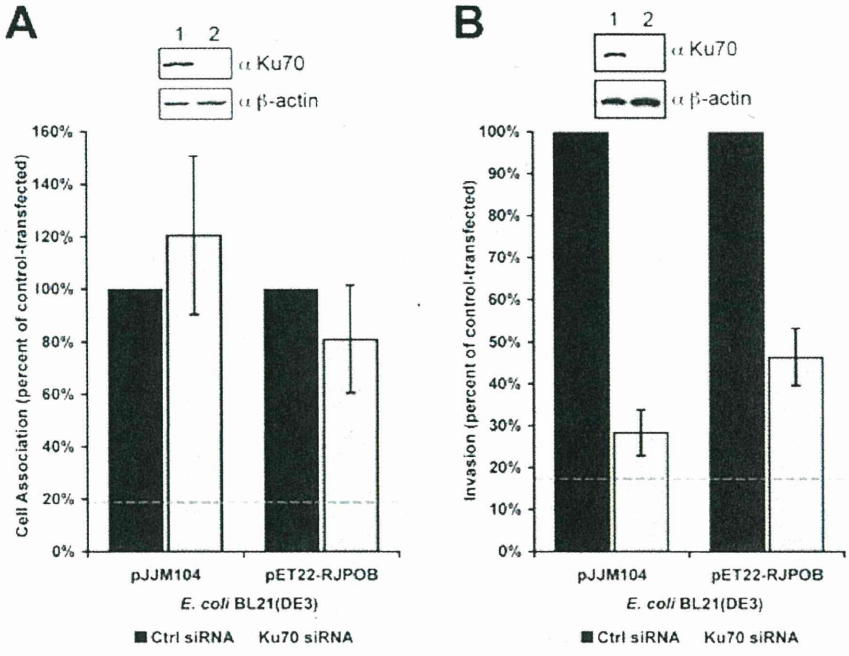

Fig. 4. rOmpB-mediated invasion of mammalian cells is dependent on Ku70 expression.
A. Effect of Ku70 siRNA depletion on rOmpB-mediated cellular association. HeLa cells transfected with irrelevant control (black bars) or Ku70 (grey bars) siRNAs were infected with *E. coli* BL21(DE3) expressing the empty vector (pET-22b) or alleles of full-length rOmpB (pJJM104 or pET22-RJPOB) and assayed for bacterial association. Dashed dark grey line shows non-specific levels of association (as a per cent of rOmpB-mediated association in control siRNA-transfected cells) seen with *E. coli* expressing the empty vector. Inset: immunoblot analysis of Ku70 protein levels in (1) control and (2) Ku70 siRNA-transfected HeLa cells. The anti-β-actin immunoblot serves as a protein loading control.
B. Effect of Ku70 siRNA depletion on rOmpB-mediated cellular invasion. HeLa cells transfected with an irrelevant control (black bars) or Ku70 (grey bars) siRNAs were infected with *E. coli* BL21(DE3) expressing the empty vector (pET-22b) or alleles of full-length rOmpB (pJJM104 or pET22-RJPOB) and assayed for bacterial invasion. Dashed dark grey line shows non-specific levels of invasion (as a per cent of rOmpB-mediated invasion in control-siRNA transfected cells) seen with *E. coli* expressing the empty vector. Inset: immunoblot analysis of Ku70 protein levels in (1) control and (2) Ku70 siRNA-transfected HeLa cells. The anti-β-actin immunoblot serves as a protein loading control.

rOmpB protein is contained within the passenger domain. To assess this hypothesis, we expressed and purified the *R. conorii* rOmpB passenger domain (aa 36–1334) fused to glutathione S-transferase (GST–$rOmpB_{36-1334}$) under native conditions (Fig. 5A). To determine whether the purified GST–$rOmpB_{36-1334}$ fusion interacts with mammalian cells, we incubated monolayers of HeLa cells with equivalent microgram quantities of either purified GST or GST–$rOmpB_{36-1334}$, washed and fixed the cells and then processed them for immunofluorescence using anti-GST antisera. As shown in Fig. 5B, GST–$rOmpB_{36-1334}$ bound to HeLa cells in a punctate staining pattern (upper panels) similar to that previously observed for plasma membrane-associated Ku70 (Martinez *et al.*, 2005). In contrast, GST alone did not bind to HeLa cells (lower panels). As we had demonstrated that GST–$rOmpB_{36-1334}$ could bind to mammalian cells, we sought to determine whether the *R. conorii* passenger domain could functionally compete for host receptor binding and prevent rOmpB-mediated cell association. As shown in Fig. 5C, pre-incubation of HeLa cells with 100 μg ml^{-1} of GST–$rOmpB_{36-1334}$, but not GST, reduced rOmpB-mediated adherence to HeLa cells. These results suggest that the recombinant purified rOmpB passenger domain is properly folded and functional. To investigate whether the purified rOmpB passenger domain could interact with Ku70, we performed protein affinity assays using detergent-solubilized HeLa cell lysates incubated with glutathione-sepharose beads coupled with either GST as a control or GST–$rOmpB_{36-1334}$. Western immunoblot analysis of elutions from these pull-down assays using anti-Ku70 antisera revealed that GST–$rOmpB_{36-1334}$, but not GST alone, interacts with Ku70 from HeLa cell lysates (Fig. 5D), in accordance with the finding that Ku70, purified from mammalian cell extracts, interacts with rOmpB from *R. conorii* lysates (Martinez *et al.*, 2005). To determine whether the interaction between $rOmpB_{36-1334}$ and Ku70 precludes any mammalian protein intermediate, we expressed and purified His-tagged $Ku70_{1-609}$ from bacterial lysates (Fig. 5E, left panel) and tested this for association with GST or GST–$rOmpB_{36-1334}$ coupled to glutathione-sepharose beads. As shown in Fig. 5E (right panel), the bacteria-derived Ku70 associates specifically with rOmpB, indicating that Ku70, in the absence of any other mammalian factors, can interact with rOmpB. Together, these

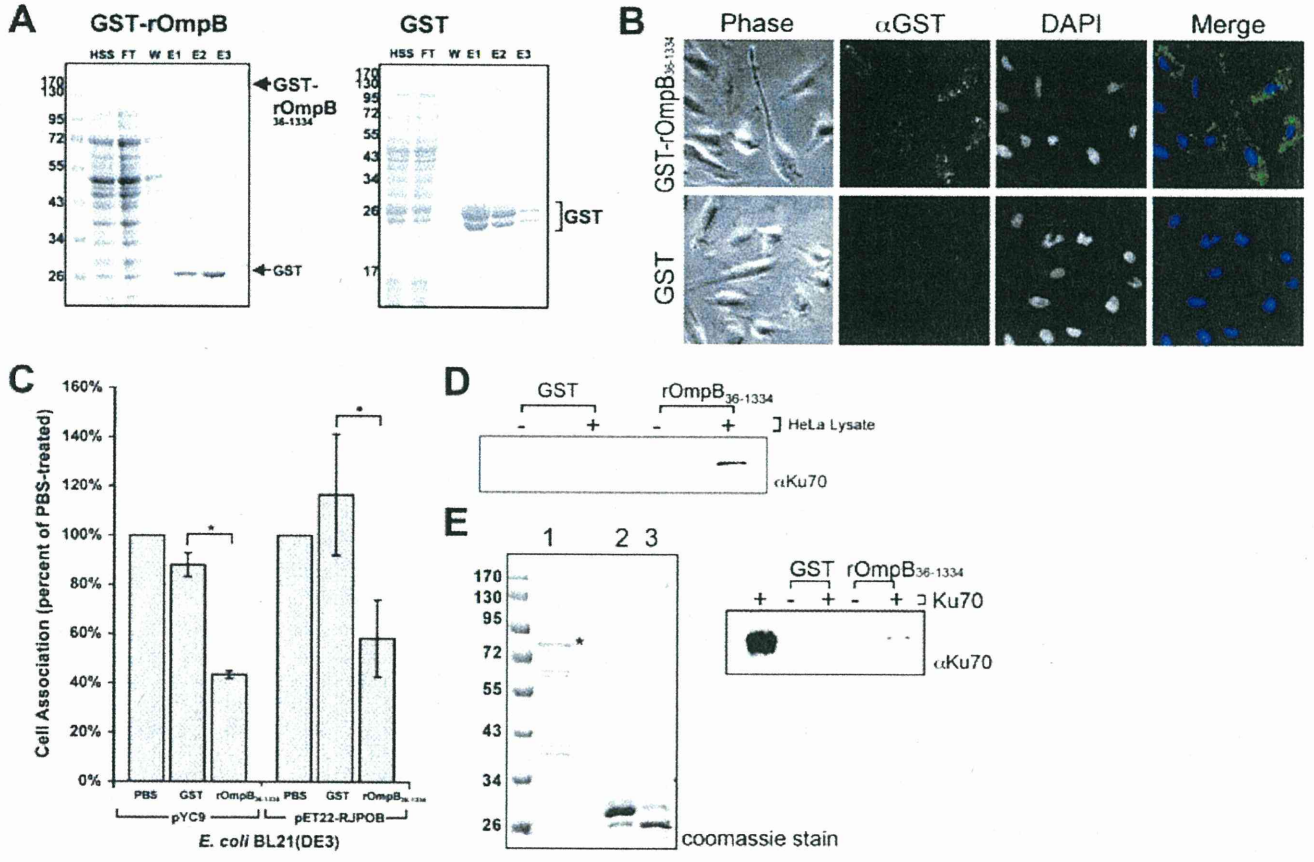

Fig. 5. The purified recombinant rOmpB passenger domain, GST-OmpB$_{36-1334}$ competitively inhibits rOmpB-mediated adherence and interacts with Ku70.

A. Coomassie-stained SDS-PAGE of GST–rOmpB$_{36-1334}$ and GST proteins expressed and purified under native conditions from the IPTG-inducible pGEX expression system in *E. coli* TOP10. Purifications were performed from bacteria harbouring the empty vector pGEX-2TKP or the gene encoding the *R. conorii* passenger domain, pGEX-*ompB*$_{106-4001}$.) Fractions shown include the cleared bacterial high-speed supernatant (HSS), flow-throw (FT), washes (W) and elutions (E1, E2 and E3).

B. Phase contrast and fluorescence micrographs of HeLa cells incubated with purified GST–rOmpB$_{36-1334}$ (top panels) or GST alone (bottom panels). Cell nuclei were stained with DAPI, and GST-tagged proteins with rabbit anti-GST and AlexaFluor 488-conjugated goat anti-rabbit IgG.

C. rOmpB-mediated adherence in the presence of exogenous GST–rOmpB$_{36-1334}$. Confluent monolayers of HeLa cells pre-incubated for 15 min with PBS, or 100 μg ml^{-1} of GST or GST–rOmpB$_{36-1334}$ in serum-free media were infected with *E. coli* BL21(DE3) expressing the *R. conorii* or *R. japonica* rOmpB allele (pYC9 and pET22-RJPOB respectively) then assayed for bacterial association. *P*-values were determined using a two-tailed Student's *t*-test, $^{*}P < 0.05$.

D. GST or GST–rOmpB$_{36-1334}$ coupled to glutathione-sepharose beads were incubated with detergent-extracted HeLa cell lysates, washed, pelleted and resolved by SDS-PAGE for analysis of Ku70 association by immunoblotting using anti-Ku70 sera.

E. Purified 10xHis-Ku70$_{1-609}$ (1) or GST (2) and GST–rOmpB$_{36-1334}$ (3) coupled to glutathione-sepharose beads were resolved by SDS-PAGE and assessed for relative purity by Coomassie staining (left panel). GST and GST–rOmpB$_{36-1334}$ coupled to glutathione-sepharose beads were incubated with 5 μg of purified 10xHis-Ku70$_{1-609}$, then washed, pelleted and resolved by SDS-PAGE. Ku70 association was determined by immunoblot analysis using anti-Ku70 mouse sera (right panel). The asterisk (*) denotes full-length recombinant Ku70 construct. Smaller species are all αHis-reactive Ku70 C-terminal truncations.

results demonstrate that the purified rOmpB passenger domain interacts with Ku70 and also competitively inhibits rOmpB-mediated bacterial association with the cell.

rOmpB–Ku70-mediated invasion is actin-dependent

Previous work had shown that *R. conorii* entry into epithelial cells involves actin cytoskeletal rearrangements at the site of bacterial contact. These actin rearrangements are thought to be a consequence of signalling through cellular protein tyrosine kinases and phosphoinositide 3-kinases leading to Arp2/3 activation (Martinez and Cossart, 2004). To investigate the involvement of actin in rOmpB-mediated invasion, HeLa cells infected for 60 min with *E. coli* BL21(DE3) expressing the *R. conorii* or *R. japonica* rOmpB alleles were stained for surface-associated *E. coli* and cellular actin, then examined by confocal fluorescence microscopy (Fig. 6A and B). In numerous cases, rOmpB-expressing *E. coli* appeared

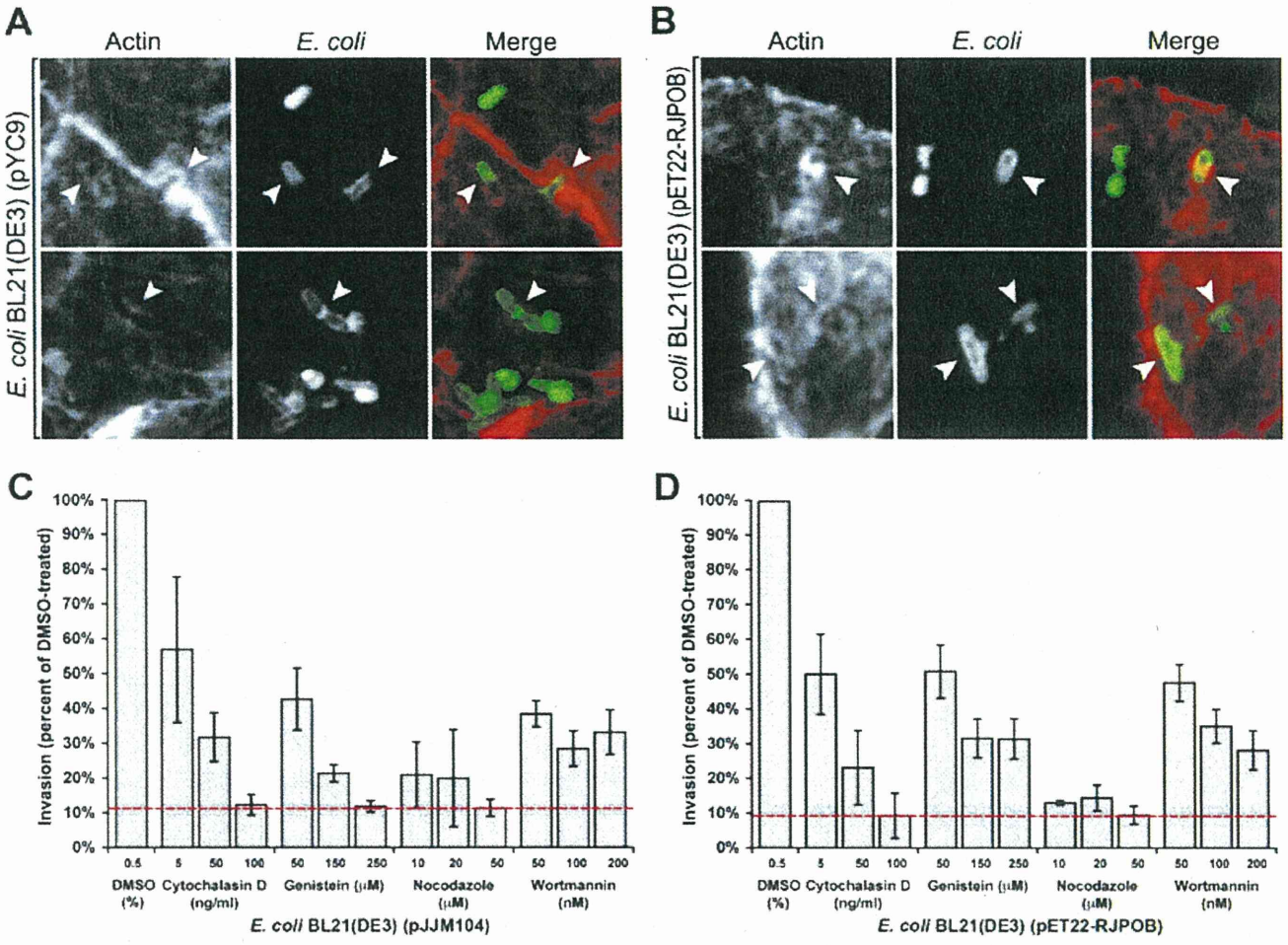

Fig. 6. Actin involvement in rOmpB-mediated invasion. HeLa cell monolayers on glass coverslips were infected for 1 h with *E. coli* BL21(DE3) expressing *R. conorii* rOmpB (pYC9) in A and *E. coli* BL21(DE3) expressing *R. japonica* rOmpB (pET22-RJPOB) in B. Cells were washed thoroughly with PBS, fixed, and then processed for immunofluorescence staining of extracellular bacteria and cellular actin. Images represent an individual confocal slice from a Z-stack capture. White arrowheads depict sites of actin recruitment around rOmpB-expressing bacteria.
C. Confluent monolayers of HeLa cells pretreated for 30 min with DMSO or inhibitors of the actin cytoskeleton (cytochalasin D), phospho-tyrosine kinases (genistein), microtubules (nocodazole) and phosphoinositide kinases (wortmannin) at the indicated concentrations were infected with *E. coli* BL21(DE3) expressing the *R. conorii* rOmpB (pJJM104), and subsequently assessed for bacterial invasion using the gentamicin protection assay. Levels of invasion are displayed as a per cent of the rOmpB-mediated invasion seen in DMSO-treated cells. Red dashed line denotes background levels of invasion seen in vector control infection.
D. HeLa cells were infected with *E. coli* BL21(DE3) expressing the *R. japonica* rOmpB (pET22-RJPOB) as described in C. Levels of invasion are displayed as a per cent of the rOmpB-mediated invasion seen in DMSO-treated cells. Red dashed line denotes invasion background seen in vector control infection.

to induce localized actin recruitment, indicated by the halo of actin around the bacterium (Fig. 6A and B, arrows).

To further query the requirement for actin in the rOmpB–Ku70-mediated invasion process, we employed pharmacological inhibitors of actin (cytochalasin D), as well as phosphotyrosine kinases (genistein), microtubules (nocodazole) and phosphoinositide 3-kinases (wortmannin), players shown to function in activation or stimulation of actin polymerization. We performed gentamicin protection assays using rOmpB-expressing *E. coli* strains and HeLa cells pretreated with either dimethylsulfoxide (DMSO) (control), or increasing concentrations of the pharmacological inhibitors, and assayed for the loss of the invasion phenotype. Neither DMSO nor the drugs at their highest concentrations appeared to affect bacterial or mammalian cell viability by colony-forming unit enumeration and trypan blue staining respectively (data not shown). As shown in Fig. 6C and D, *R. conorii* and *R. japonica* rOmpB-mediated invasion of HeLa cells was inhibited in a concentration-dependent manner, in cells treated with cytochalasin D and genistein, in most cases reducing invasion to levels observed of the non-invasive control (Fig. 6A and B, red dashed line). Cells treated with increasing concentrations of wortmannin exhibited only an intermediate inhibitory effect on invasion, reminiscent of that seen in *R. conorii* infections (Martinez and Cossart, 2004).

Previous studies had implicated microtubule dynamics as playing a critical role in uptake of invasive 'zippering' pathogens, such as *Campylobacter jejuni* (Biswas *et al.*, 2003) and in regulating Arp2/3-mediated actin cytoskeletal changes (Campellone *et al.*, 2008). We therefore, investigated whether inhibition of microtubule stability would affect rOmpB-mediated invasion of HeLa cells. A shown in Fig. 6C and D, destabilization of the cells' microtubule cytoskeletal infrastructure with nocodazole reduced rOmpB–Ku70-mediated invasion to levels similar to the non-invasive control (dashed line in Fig. 6C and D). The comparable effects on invasion seen between *E. coli* expressing the *R. conorii* and *R. japonica* rOmpB allele suggests rOmpB may stimulate entry similarly among related rickettsial species. Furthermore, the mechanism for rOmpB–Ku70-mediated internalization correspondingly mirrors that previously observed in the *R. conorii* invasion process (Martinez and Cossart, 2004). Taken together, these results suggest that the integrity of actin and microtubule cytoskeletal structures is crucial for rOmpB-mediated invasion.

c-Cbl, clathrin, caveolin-2, but not caveolin-1, are involved in rOmpB-mediated entry

Recent studies have shown that many pathogens, including *Listeria monocytogenes* and *Yersinia pseudotuberculosis*, utilize the 'zippering' pathway of invasion, highjacking the clathrin-, caveolin- and ubiquitin-mediated endocytosis of host receptors to gain access to the nutrient-rich intracellular environment of mammalian host cells (Veiga and Cossart, 2005; Bonazzi and Cossart, 2006; Hamon *et al.*, 2006). Invasion of 'zippering' bacteria into non-phagocytic mammalian cells is therefore a combination of signalling events leading to localized actin rearrangements at entry foci coupled with the endocytosis of host cell receptors (Veiga *et al.*, 2007). Previous studies have also demonstrated that the E3 ubiquitin ligase c-Cbl-mediated ubiquitin modification of Ku70 correlates with *R. conorii* entry (Martinez *et al.*, 2005) and that rOmpB is sufficient to mediate invasion of non-phagocytic mammalian cells (Uchiyama *et al.*, 2006). As ubiquitin modification of Ku70 appears to be an important event during rickettsial entry, we first determined the contribution of c-Cbl to the rOmpB-dependent entry process using siRNAs against endogenous human c-Cbl. As shown in Fig. 7A, inhibition of endogenous c-Cbl expression in HeLa cells reduced rOmpB-mediated uptake to levels similar to those observed for cells treated with Ku70 siRNA.

A recent study has demonstrated that the InlB-mediated invasion of *L. monocytogenes* involves the sequential recruitment of clathrin and actin, respectively, to entry foci and that the recruitment of clathrin is required for the localized actin rearrangements involved in efficient bacterial entry (Cossart and Veiga, 2008). We next determined whether major components of the endocytic pathway also contribute to rOmpB-mediated invasion. As shown in Fig. 7B, transfection of siRNAs directed against caveolin-1, caveolin-2 and clathrin heavy chain were able to reduce endogenous expression of these proteins. Interestingly, rOmpB-mediated invasion of HeLa cells was diminished in cells transfected with siRNAs against caveolin-2 and clathrin heavy chain, but not caveolin-1, suggesting that rOmpB-mediated uptake is independent of caveolin-1 (Fig. 7B). Together, these results suggest a role for c-Cbl, clathrin and caveolin 2-mediated endocytosis in the entry of rOmpB-expressing bacteria into non-phagocytic mammalian cells.

Discussion

The ability of SFG rickettsiae to bind to and invade target mammalian cells is a critical initial event during pathogenesis. A previous report identified a mammalian protein, Ku70, as a receptor involved in *R. conorii* invasion and had identified the rickettsial autotransporter protein, rOmpB, as a ligand (Martinez *et al.*, 2005). These results suggested that the interactions between Ku70 and rOmpB are important to initiate signals leading to rickettsial uptake. Here we demonstrate that rOmpB from both *R. conorii* and the closely related SFG rickettsia, *R. japonica*, are sufficient to mediate invasion of non-phagocytic mammalian cells in a Ku70-dependent manner.

rOmpB is an abundant surface protein expressed by rickettsiae and exhibits homology to a family of modular proteins in Gram-negative bacteria called autotransporters (Blanc *et al.*, 2005). We have shown that rOmpB from *R. conorii*, when expressed in *E. coli*, can mediate association to and invasion of non-phagocytic mammalian cells. A previous study has suggested that the rOmpB β-peptide domain may serve as a rickettsial adhesin (Renesto *et al.*, 2006); our results indicate that the passenger domain also functions in cellular recognition and may also be responsible for adherence to target cells. While rOmpB from *R. conorii* and *R. japonica* presumably interact with multiple eukaryotic ligands at the plasma membrane, our findings suggest that interactions with Ku70 are integral in the invasion process. Given the high degree of shared sequence identity and homology in the passenger domains of rOmpB molecules expressed by closely related and divergent rickettsia (Blanc *et al.*, 2005), we propose that Ku70 is likely utilized by multiple rickettsial species to gain entry into non-phagocytic mammalian cells and that disruption of this interaction in part can block invasion.

The importance of rOmpB in rickettsial pathogenesis was highlighted by the observation that anti-rOmpB anti-

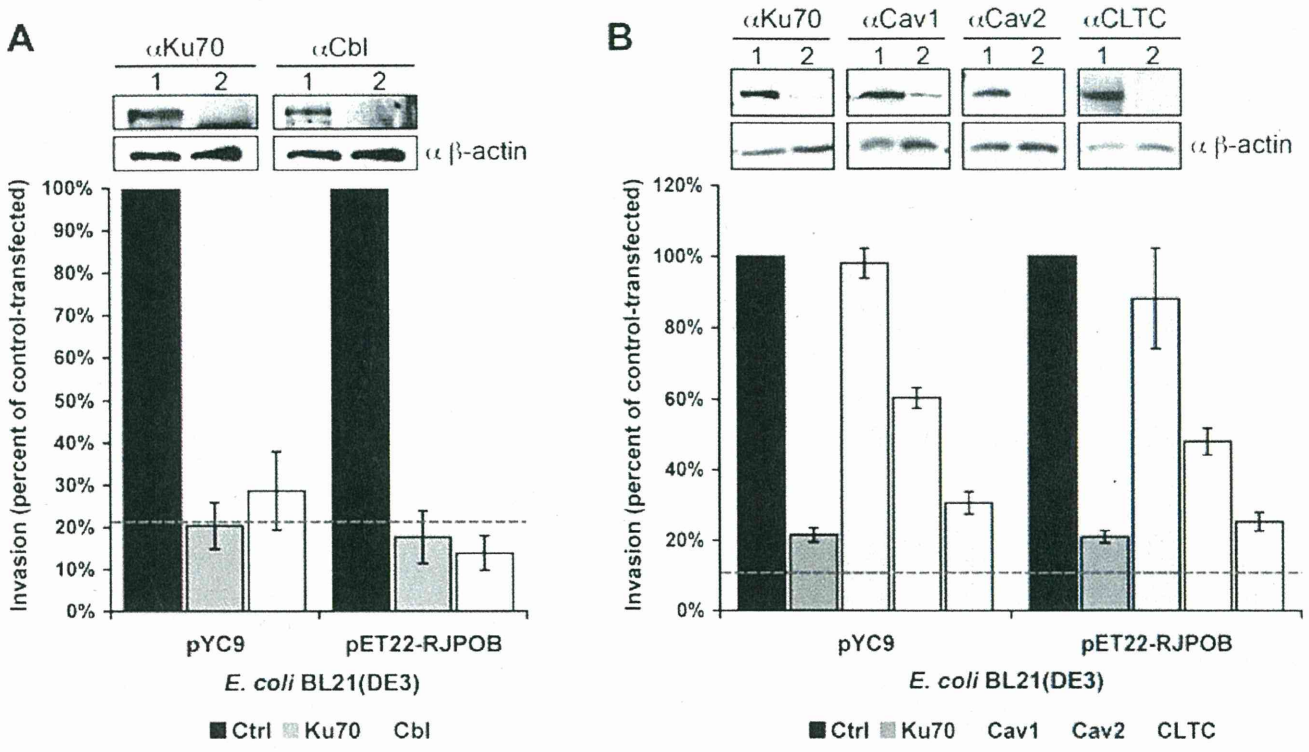

Fig. 7. rOmpB-mediated invasion of mammalian cells is dependent on c-Cbl, clathrin and caveolin-2.
A. Effect of c-Cbl siRNA depletion on rOmpB-mediated invasion. HeLa cells transfected with control (black bars), Ku70 (grey bars), or c-Cbl (white bars) siRNAs were infected with *E. coli* BL21(DE3) harbouring the empty vector (pET-22b) or rOmpB (pYC9 or pET22-RJPOB) and assayed for bacterial invasion by the gentamicin protection assay. Invasion levels are displayed as per cent of rOmpB-mediated invasion in control siRNA-transfected cells. Dark grey dashed line represents background invasion levels seen in *E. coli* expressing the empty vector. Inset: immunoblot analysis of Ku70 (left-top panel) or c-Cbl (right-top panel) protein levels in cells transfected with (1) control or (2) gene-specific siRNAs. Anti-β-actin immunoblots (bottom panels) were used as a protein loading control.
B. Effect of caveolin-1, caveolin-2, and clathrin heavy chain siRNA depletion on rOmpB-mediated invasion. HeLa cells transfected with control (black bars), Ku70 (dark grey bars), caveolin-1 (Cav1, light grey bars), caveolin-2 (Cav2, white bars) or clathrin heavy chain (CLTC, cross-hatched bars) siRNAs were infected with *E. coli* BL21(DE3) harbouring the empty vector or rOmpB (pYC9 or pET22-RJPOB) and assayed for bacterial invasion by the gentamicin protection assay. Inset: immunoblot analysis of Ku70 (first-top panel), Cav1 (second-top panel), Cav2 (third-top panel) and CLTC (fourth-top panel) protein levels in cells transfected with (1) control or (2) gene-specific siRNAs. Anti-β-actin immunoblots (bottom panels) were used as a protein loading control.

bodies protect mice from an otherwise lethal challenge of *R. conorii* (Feng *et al.*, 2004a,b) in a model of Mediterranean spotted fever. Interestingly, anti-rOmpB antisera raised against *R. conorii* rOmpB protein are cross protective against a closely related SFG rickettsia, *R. rickettsii,* and a phylogenetically divergent rickettsia, *R. australis* (Stenos and Walker, 2000; Feng and Walker, 2003; Feng *et al.*, 2004b) likely due to the high degree of sequence identity shared among rOmpB molecules. A previous study demonstrated that antisera against a specific region in the *R. rickettsii* rOmpB passenger domain (aa 451–1308) elicited protective humoral immunity in a murine model of infection. In contrast, antisera raised against part of the predicted rOmpB β-peptide (aa 1335–1704) were not protective (Diaz-Montero *et al.*, 2001). A corresponding subregion in the *R. conorii* rOmpB passenger domain (aa 545–848) is involved in the activation of effector CD8+ T-cells (Li *et al.*, 2003). We have shown that a purified GST–rOmpB$_{36-1334}$ passenger domain fusion binds to Ku70 in a biochemical pull-down assay. We have also demonstrated that GST–rOmpB$_{36-1334}$ binds to mammalian cells in a punctate pattern, and competitively inhibits *R. conorii* and *R. japonica* rOmpB-mediated adherence. Interestingly, a previous report showed that the *R. conorii* rOmpB passenger domain, but not the β-peptide, interacts with the Ku70 N-terminal domain (aa 1–535) (Martinez *et al.*, 2005) and that a monoclonal antibody (mAb) directed against an exposed Ku70 epitope (aa 506–541) does not block *R. conorii* attachment to cells, but effectively blocks internalization. We predict that a surface-exposed rOmpB domain is likely involved not only in eliciting protective immune responses, but also in recognizing Ku70. Identification of the domains involved in rOmpB–Ku70 interactions will be crucial to the development of novel anti-rickettsial therapies.

Numerous studies have implicated that entry of *R. conorii* morphologically and mechanistically resembles a zipper-like invasion strategy (Teysseire *et al.*, 1995;

Gouin *et al.*, 1999), similar to that utilized by *L. monocytogenes*, *Yersinia enterocolitica* and uropathogenic *E. coli*. In this mechanism, invasion is mediated by the sequential interactions of specific bacterial ligands and host receptors that lead to localized actin recruitment and 'zippering' of the plasma membrane around the bacterium (Cossart and Sansonetti, 2004). Previous work had also shown that the entry of *R. conorii* into non-phagocytic mammalian cells requires the activation of host signalling pathways, involving the tyrosine phosphorylation of host proteins, the activation of protein tyrosine kinases (c-Src) and the activation of lipid kinases (phosphoinositide 3 kinase), ultimately leading to localized Arp2/3-driven actin polymerization (Martinez and Cossart, 2004). Our pharmacological inhibitor studies show that rOmpB-mediated uptake closely parallels that of *R. conorii*, suggesting that rOmpB is sufficient to trigger these signalling pathways leading to bacterial entry. Interestingly, inhibition of microtubule dynamics by nocodazole treatment also inhibited rOmpB-mediated invasion of mammalian cells, as has been previously observed for the invasive, 'zippering' pathogen, *Campylobacter jejuni* (Biswas *et al.*, 2003). Exactly how microtubule and actin rearrangements could be regulated in the uptake process is unclear; however, a recent report identified a modular protein in mammalian cells termed WHAMM (WASP homologue associated with actin, membranes and microtubules) that can bind to microtubules and promote membrane tubulation and stimulate Arp2/3-mediated actin rearrangements (Campellone *et al.*, 2008). Disruption of microtuble integrity with nocodazole may also indirectly disrupt the regulation of Arp2/3-mediated actin rearrangements that are crucial for invasion of mammalian cells. The mechanism by which microtuble dynamics and actin rearrangements are regulated during bacterial invasion warrants further investigation.

Recent evidence has shown that zippering invasive pathogens can also highjack the host cellular endocytic machinery to gain entry into non-phagocytic cells (Veiga and Cossart, 2005). For example, the invasive pathogen, *Listeria monocytogenes*, induces the mono-ubiquitination of receptors – hepatocyte growth factor receptor (HGFR) (Veiga and Cossart, 2005) and E-cadherin and triggers the recruitment of clathrin and caveolin-1 to entry foci (Bonazzi and Cossart, 2006; Veiga *et al.*, 2007). Mechanistic similarities between the entry of *L. monocytogenes* and *R. conorii* suggested that ubiquitin modification of mammalian proteins, including the receptor Ku70, may also be important during SFG rickettsia invasion. Martinez and coworkers showed that *R. conorii* induces a rapid ubiquitination of Ku70 and that inhibition of the E3 ubiquitin ligase c-Cbl by siRNAs reduces *R. conorii* entry into HeLa cells (Martinez *et al.*, 2005). These results suggested that c-Cbl-mediated ubiquitination of Ku70 may be a critical signalling intermediate in *R. conorii* entry (Martinez *et al.*, 2005). Using siRNAs, we confirmed that rOmpB-mediated entry is dependent on c-Cbl. Whether rOmpB is sufficient to mediate Ku70 ubiquitination during the entry process is currently being investigated. We also determined that rOmpB-mediated invasion was in part dependent on clathrin and caveolin-2. In contrast to that observed for InlA-mediated uptake of *L. monocytogenes* (Bonazzi and Cossart, 2006), inhibition of caveolin-1 had little effect on rOmpB-mediated invasion of HeLa cells. Interestingly, the entry of non-zippering pathogens, *Salmonella typhimurium* and *Shigella flexneri*, was found to be independent of clathrin (Bonazzi and Cossart, 2006), suggesting that pathogens have evolved alternate strategies to gain access to the intracellular environment. These data support clathrin-mediated endocytosis as a general mechanism usurped by zippering pathogens to enter non-phagocytic mammalian cells and suggest that distinct utilization of caveolin-1- and caveolin-2-dependent pathways may be attributed to differences in receptor utilization. Interestingly, a recent report demonstrated that the InlB-mediated invasion of *L. monocytogenes* requires a sequential recruitment of clathrin and actin to entry foci. Inhibition of clathrin expression by siRNA transfection disrupted the recruitment of actin to sites of entry suggesting that clathrin recruitment is required for the activation of actin rearrangements (Cossart and Veiga, 2008). Taken together, these results suggest that stimulation of signals at the level of the plasma membrane receptor may be co-ordinated not only to recruit and activate components of the host cell endocytic machinery but also to recruit localized actin to sites of bacterial attachment, ultimately leading to bacterial internalization of 'zippering' pathogens.

Although ubiquitously expressed in mammalian cells, Ku70 has been found associated with the plasma membrane in high abundance on a subset of cell types, including endothelial cells, macrophages, solid tumours under hypoxic conditions and tumour cell lines, including HeLa and Vero (Muller *et al.*, 2005). Endothelial cells represent the major target cell for SFG rickettsia *in vivo* and we suggest that rickettsia have evolved a mechanism to bind to and utilize the abundant protein, Ku70, at the plasma membrane to trigger internalization. A recent study demonstrated that plasma membrane-associated Ku70 plays an important role in cell–cell adhesion and in the attachment of cells to some extracellular matrix proteins (Monferran *et al.*, 2004b). However, little else is known about the function and the regulation of Ku70 at the plasma membrane. In the absence of recognizable protein interacting motifs, such as SH2 and SH3 domains, present in other mammalian receptors, it is difficult to rationalize how Ku70 can transmit signals eventually leading to bacterial uptake. One hypothesis is that Ku70

may interact with other surface proteins to facilitate rickettsial entry. Through yeast two-hybrid screens, several groups have identified Ku70 interactors, including, matrix metalloprotease nine, a protein that plays a central role in wound healing, angiogenesis, arthritis and tumour metastasis (Monferran *et al.*, 2004a) and the ADP-ribosylation factor 6, a small GTP-binding protein that regulates membrane traffic and the actin cytoskeleton at the plasma membrane (Schweitzer and D'Souza-Schorey, 2005). In addition, under certain conditions, Ku70 was found to associate with the epidermal growth factor receptor on mammalian cells (Bandyopadhyay *et al.*, 1998), although the significance of this interaction to Ku70 function remains unclear. Whether these proteins play a role in rickettsia entry is currently being investigated. Interestingly, a recent report elucidated a critical role for non-muscle myosin IIA (NMMIIA) in the transport of a nuclear protein, nucleolin, to the plasma membrane where nucleolin can then interact with various ligands (Huang *et al.*, 2006). NMMIIA is an actin motor protein involved in the modulation of the actinomyosin cytoskeleton and regulating cell-shape, changes in cell migration, secretion or cell division (Sellers, 2000). As actin polymerization plays a crucial role in rOmpB-mediated internalization, one possibility is that NMMIIA aids in modulating actin contractility at the endocytic cup. Alternatively, NMMIIA may be involved in the trafficking of Ku70 to the plasma membrane, similar to that observed with nucleolin. Interactions of rOmpB with Ku70 may trigger signalling events that couple actin rearrangements and recruitment of components of the endocytic machinery to entry foci. The potential role of this myosin in rickettsial entry is intriguing and warrants further investigation.

Our results underscore the importance of rOmpB and Ku70 in the rickettsia entry process. However, recent data suggest that other host cell receptors and rickettsia ligands likely also play important roles in the adherence and invasion of mammalian cells. Several studies have illustrated the importance of another related rickettsia autotransporter protein, rOmpA, in the attachment to host cells and in the generation of protective humoral immune responses (Anacker *et al.*, 1987a,b; Li *et al.*, 1988; Li and Walker, 1998). Sequence data mining revealed the presence of a gene family termed *sca* within different SFG rickettsial genomes whose genes are predicted to encode either secreted proteins or outer membrane proteins (Blanc *et al.*, 2005). Although many genes appear to be fragmented or split, several genes, including *ompB*, are present in nearly all SFG rickettsiae (Roux and Raoult, 2000; Blanc *et al.*, 2005), suggesting that they may play important roles in rickettsial pathogenesis. Elucidating the functions of rOmpB in addition to conserved Sca proteins is crucial to understanding the complex host–pathogen interaction underlying successful SFG rickettsia infections in human hosts and may lead to the development of more efficacious therapies.

Experimental procedures

Cell lines and bacterial strains

HeLa cells (ATCC, Manassas, VA) and Vero cells were grown in Dubecco's modified Eagle's medium (DMEM) supplemented with 10% heat-inactivated fetal bovine serum, 1× nonessential amino acids (Lonza, Walkersville, MD) and 0.5 mM sodium pyruvate. Cells were grown at 37°C/5% CO_2. *E. coli* BL21(DE3) or TOP10 were grown in Luria–Bertani (LB) Miller broth at 37°C supplemented with ampicillin (100 μg ml^{-1}) where appropriate. Bacteria were diluted 1:20 from overnight cultures, grown to an OD_{600} = 0.6, and induced with 100 μM IPTG for 3 h at 37°C or as otherwise indicated.

Antibodies and other reagents

For immunoblot detection, the anti-Ku70 mAb (N3H10) was purchased from NeoMarkers (Fremont, CA). Anti-clathrin mAb (CHC5.9) was purchased from Chemicon International (Temecula, CA). The anti-6xHis rabbit polyclonal was obtained from Covance (Berkeley, CA). Anti-GST rabbit sera (Z-5) was purchased from Santa Cruz Biotechnology (Santa Cruz, CA). The anti-c-Cbl and anti-caveolin-1 rabbit polyclonals were purchased from Cell Signaling Technology (Danvers, MA). Anti-caveolin-2 rabbit antisera and the polyclonal goat anti-mouse IgM horseradish peroxidase (HRP) conjugate were purchased from Abcam (Cambridge, MA). The anti-actin mAb (AC-15), rabbit anti-mouse IgG HRP conjugate and goat anti-rabbit IgG HRP conjugate used for western immunoblot analysis; the pharmacological inhibitors, cytochalasin D, genestein, nocodazole and wortmannin were purchased from Sigma (Saint Louis, MO). AlexaFluor 488-conjugated goat anti-rabbit IgG and Cell Tracker Red CMTPX, used in immunofluorescence studies, and the pCR2.1 TOPO TA Cloning kit were purchased from Invitrogen (Carlsbad, CA). The gentamicin sulfate was purchased from MP Biomedicals (Solon, OH). Annealed siRNAs against caveolin-1 sense strand 5′-CGAAAUACUGGUUUUACCGtt-3′ and antisense strand 5′-CGGUAAAACCAGUAUUUCGtc-3′; caveolin-2 sense strand 5′-GCACACAACGAUUAUAGUAtt-3′ and antisense strand 5′-UACUAUAAUCGUUGUGUGCtt-3′; c-Cbl sense strand 5′-CCUUAUAUCUUAGACCUGCtt-3′ and antisense strand 5′-GCAGGUCUAAGAUAUAAGGtg-3′; clathrin heavy chain sense strand 5′-GGGAAGUUACAUAUUAUUGtt-3′ and antisense strand 5′-CAAUAAUAUGUAACUUCCCtc-3′; Ku70 sense strand 5′-GGCUAUGUUUGAAUCUCAGtt-3′ and antisense strand 5′-CUGAGAUUCAAACAUAGCCtt-3′; and the Silencer negative control #1 siRNA were obtained from Ambion (Austin, TX). Complete protease inhibitor cocktail was purchased from Roche (Indianapolis, IN). Glutathione-sepharose 4B beads used in GST purifications were purchased from Amersham Biosciences (Piscataway, NJ). Chemically competent *E. coli* BL21(DE3) were attained from Stratagene (La Jolla, CA). The QIAquick Spin Kit was obtained from Qiagen (Valencia, CA). The pET-22b vector was purchased from Novagen (Gibbstown, NJ). Restriction enzymes BamHI, NcoI, XhoI and KpnI were all obtained from New England BioLabs (Ipswich, MA).

Table 1. Plasmids.

Plasmid	Description	Source
pET22-RJPOB	pET-22b, *R. japonica ompB*	Uchiyama *et al.* (2006)
pET-22b		Novagen
pGEX-2TKP		T. Kouzarides
pJJM104	pET-22b, *R. conorii* $ompB_{3-4965}$	This work
pYC9	pET-22b, *R. conorii* $ompB_{106-4965}$	This work
pYC11	pGEX-2TKP, *R. conorii* $ompB_{106-4001}$	This work
pYC30	pET-16b, *Homo sapiens* $XRCC6_{1-1827}$ (Ku70)	This work

Plasmid DNA constructs

ompB fragments were amplified by polymerase chain reaction (PCR) from a chromosomal preparation of *R. conorii* Malish 7 containing the *ompB* gene (GenBank Accession No. AAL03623). All constructs were initially cloned into pCR2.1 (Invitrogen), digested, gel-purified using the QIAquick Spin Kit (Qiagen) before being inserted into its expression vector. Plasmids used in this study are listed in Table 1. The full-length *ompB* was PCR amplified using the primers GAGCCCGGATCCAGCTCAAAAAC CAAATTTTCT and GGCTCGAGGAAGTTTACACGGACTTTT AG and inserted into pET-22b (BamHI and XhoI sites) generating pJJM104. The plasmid pYC9, encoding the full-length *R. conorii* rOmpB excluding its endogenous signal peptide, was generated by PCR amplification of *ompB* from the chromosome using the primers ACCATGGCTATACAGCAGAATAGAAC and GGCTC-GAGGAAGTTTACACGGACTTTTAG, then digested and ligated into pET-22b (NcoI and XhoI). The region of *ompB* encoding the passenger domain of the protein was PCR amplified using the primers ACCATGGCTATACAGCAGAATAGAAC and GGCTC GAGTAATCTGTTACCAAGTTGAGC, digested (NcoI and XhoI) and ligated into pGEX-2TKP (gift from Dr T. Kouzarides, UK Gurdon Institute), generating pYC11. The plasmid pYC30, encoding a 10xHis-$Ku70_{1-609}$, was generated by excision of $XRCC6_{1-1827}$ from pYC29 (NdeI and XhoI) and ligation into pET-16b (NdeI and XhoI).

E. coli *fractionation*

One hundred millilitres of induced *E. coli* BL21(DE3) cultures was pelleted and resuspended in 10 ml 20 mM Tris (pH 8) containing 1× protease inhibitor (Roche). Cells were passed twice through the French Pressure cell (1500 psi) and cleared by centrifugation at 10 000 *g* for 5 min. Inner membrane proteins were extracted by incubation with sarkosyl (final concentration of 0.5%) at room temperature for 15 min. Outer membranes were pelleted by ultracentrifugation (SW40Ti, 32 000 r.p.m., 30 min, 4°C) and resuspended in 2× sample buffer. Whole cell lysates, soluble/sarkosyl-solubilized and outer membrane fractions were resolved by SDS-PAGE and analysed by immunoblotting with anti-6xHis rabbit sera (Covance) and goat anti-rabbit HRP conjugate (Sigma).

Cell association and invasion assays

Cell association and invasion assays were performed as described (Martinez *et al.*, 2000). Briefly, HeLa cells were seeded into 24 well plates at 1.2×10^5 cells per well 24 h prior to infection. Prior to infection, the cells were washed three times with serum-free DMEM and the medium was replaced with 950 µl of pre-warmed serum-free DMEM. Triplicate wells were then infected with 50 µl of induced bacteria ($OD_{600} = 1.0$) resuspended in phosphate-buffered saline (PBS). Bacterial contact with host cells was initiated by centrifugation of the plates at 200 *g* for 5 min. Plates were incubated at 37°C/5% CO_2 for 20 or 60 min to assess for cell association and invasion respectively. In cell association assays, cells were washed five times with PBS or serum-free DMEM, then lysed with 1 ml 0.1% Triton X-100 in *dd*H_2O and plated onto LB agar plates for colony-forming units. Adherence frequencies were calculated as the per cent of cell-associated bacteria recovered after the PBS washes out of the total bacteria in each well after the 20 min incubation. To determine bacterial invasion, cells were washed three times with PBS or serum-free DMEM following the 1 h incubation period, then incubated for an additional 2 h with 100 µg ml^{-1} of gentamicin sulfate (MP Biomedicals) in complete DMEM. Thereafter, cells were washed three times with PBS, then lysed with 0.1% Triton X-100 in *dd*H_2O and plated onto LB agar plates. Invasion frequencies were determined as the number of bacteria surviving the gentamicin challenge out of the total bacterial input following the initial 1 h incubation. In inhibitory assays, cell association and invasion were subsequently normalized as a per cent relative to the infections of mock-treated cells. Infections were done in triplicate and results are representative of at least three experiments. *P*-values were determined by a two-tailed Student's *t*-test on replicates from a single experiment.

Electron microscopy

For scanning electron microscopy, HeLa cells grown on 12 mm glass coverslips in 24 well plates were infected with 10 µl of induced bacteria ($OD_{600} = 1.0$) for 1 h, washed, then fixed for 20 min with 4% paraformaldehyde (PFA) in PBS, followed by fixation in 2.5% glutaraldehyde in PBS for an additional 72 h. Samples were next serially dehydrated with increasing concentrations of ethanol, critical point dried with hexamethyldisilazane, then sputter coated with 80% platinum/20% palladium to 8 nm by Cressington Sputter Coater 208HR. The samples were visualized using Fei NovaNano SEM200 at a distance of 5 mm. For transmission electron microscopy, HeLa cells grown in 6 well plates (3×10^5 cells per well) were infected with 2 ml of induced bacteria ($OD_{600} = 2.0$) for 2 h, washed, and then bathed in fixative (2% glutaraldehyde, 4% PFA, 0.1 M sodium cacodylate buffer). Cells were carefully scraped from the plate, pelleted at 500 *g* for 5 min, allowed to fix overnight at 4°C, then post-fixed with 1% OsO_4 in 0.1 M sodium cacodylate buffer for 60 min. The samples were stained in 1% uranyl acetate in maleate buffer for 60 min, and then serially dehydrated with increasing concentrations of ethanol. Cells were embedded in spurr resin for 48 h at 60°C, thin

sectioned (90 nm) using a Reichert-Jung Ultracut device and then post-stained in uranyl acetate and lead citrate. The samples were imaged on the FEI Tecnai F30 with a Gatan charge-coupled device (CCD) digital micrograph.

RNA interference assays

SiRNA transfections were done as previously described (Martinez *et al.*, 2005). Briefly, HeLa cells plated in 6 well plates at 1.2×10^5 cells per well were transfected with 10 nM of the indicated siRNA (Ambion) using Oligofectamine transfection reagent (Invitrogen), as recommended by the manufacturer. Forty-eight hours post transfection, cells were split into 24 well plates at 1.2×10^5 cells per well. Cells were tested for cell association, invasion and protein levels 72 h post transfection. Protein levels were assessed by immunoblot analysis of cell lysates; anti-Ku70 mAb (N3H10, 200 ng ml^{-1}), antic-Cbl rabbit sera (1:1000), anti-β actin mAb (AC-15, 1:20 000), anti-clathrin (CHC5.9, 1:100), anti-caveolin-1 (1:1000), anti-caveolin-2 (1 μg ml^{-1}).

Pharmacological inhibitor assays

HeLa cells plated in 24 well plates at 1.2×10^5 cells per well were washed and starved in serum-free DMEM for 1 h. Thirty minutes prior to infection, the HeLa cells were incubated in 950 ml of serum-free DMEM containing the cytochalasin D (Sigma), genistein (Sigma), nocodazole (Sigma) or wortmannin (Sigma) at the indicated concentrations, or DMEM with 0.5% (v/v) DMSO as a mock-treated control. We assessed cell viability by performing trypan blue staining on drug-treated cells. Bacterial viability was assessed by comparing colony-forming units of bacteria following 1 h incubation in DMEM, DMSO or the pharmacological inhibitor at the highest utilized concentration.

Protein purification

Expression and purification of rOmpB$_{36-1334}$ under native conditions was done utilizing the pGEX prokaryotic expression system. Protein expression was done in *E. coli* TOP10 strains (Invitrogen) carrying the pGEX derivatives. Overnight cultures were diluted 1:20 into 1 l of fresh medium and grown at 37°C to mid-exponential phase. Cultures were cooled to 30°C and induced using 10 μM IPTG at 30°C for 4–6 h. Bacteria were harvested by centrifugation, resuspended in PBS containing protease inhibitor, and lysed by passing through the French pressure cell 2× (1500 psi). Lysates were cleared by ultracentrifugation (SW40Ti, 32 000 r.p.m., 1 h, 4°C) and purified by gravity flow over glutathione-sepharose beads (Amersham Biosciences), and eluted using 20 mM glutathione in PBS. Purified protein was dialysed into PBS with 10% glycerol, then snap-frozen in liquid nitrogen and stored at −80°C. Expression of 10xHis-Ku70$_{1-609}$ was done in *E. coli* BL21(DE3). Following induction using 1 mM IPTG at 37°C for 4 h, bacteria were harvested by centrifugation and lysed in lysis buffer (20 mM NaH_2PO_4, 0.5 M NaCl, 20 mM imidazole, pH 7.4) using the French pressure cell as described above. Lysates were cleared by ultracentrifugation (SW40Ti, 32 000 r.p.m., 1 h, 4°C) and loaded onto a 5 ml HisTrap-FF column (GE Healthcare) using an ÄKTA FPLC with UPS-900 UV absorbance monitor and Frac920 fraction collector (GE Healthcare). The column was washed with 18 column volumes (CV) of lysis buffer, 5 CV 125 mM imidazole lysis buffer and then eluted over 6 CV using a linear gradient of 125–500 mM imidazole-containing lysis buffer. Fractions containing 10xHis-Ku70$_{1-609}$ were pooled and dialysed into 10% glycerol-PBS, then snap-frozen in liquid nitrogen and stored at −80°C.

Glutathione bead pull-down assays

Glutathione-sepharose beads (Amersham Biosciences) coupled to GST or GST–rOmpB$_{36-1334}$ were added to either 1% NP-40 lysis buffer (1% NP-40, 20 mM Tris pH 8.0, 150 mM NaCl, 10% glycerol, 1× complete protease inhibitor), cleared HeLa cell lysates from a confluent 10 cm dish extracted with 1% NP-40 lysis buffer or 5 μg of purified 10xHis-Ku70$_{1-609}$ in 300 μl 1% NP-40 lysis buffer. Bead-protein mixtures were rocked at 4°C for 2 h, pelleted and washed three times with NP-40 lysis buffer. The supernatants were then aspirated and the beads were boiled in sample buffer for SDS-PAGE analysis.

Immunofluorescence

To assess for surface expression of rOmpB on *E. coli* BL21(DE3), 200 μl of bacterial culture diluted in PBS (OD_{600} = 0.05) was applied to L-polylysine-coated coverslips in a 24 well plate and centrifuged at 200 *g* for 10 min to induce contact. Bacteria were then fixed with 4% PFA in PBS for 20 min, washed to remove unassociated bacteria, and allowed to air dry. Bacteria were next rehydrated in PBS for 5 min, then blocked in 2% BSA-PBS for 1 h. *E. coli* were stained for rOmpB by incubation with anti-Rc7 rabbit hyper-immune sera against heat-killed rickettsia (1:200) in 2% BSA-PBS for 1 h, washed three times with PBS, followed by a 1 h incubation in the dark with AlexaFluor 488-conjugated goat anti-rabbit IgG (1:1000), and propidium iodide (10 μM) to detect membrane-compromised bacteria. Coverslips were washed three times with PBS, and then mounted with mowiol onto slides. Images were captured on an Olympus AX-70 fluorescence microscope coupled to a CCD camera at 1000× magnification. Images were assembled in Adobe Photoshop.

In cell association assays, following infection in 24 well plates (described under *Cell association and invasion assays*), cells were washed and fixed with 4% PFA at room temperature for 20 min. To assess for total association of *E. coli*, cells were permeabilized with 0.1% Triton X-100 in PBS and subsequently stained for total *E. coli* with rabbit anti-*E. coli* antisera (1:1000) in 2% BSA-PBS for 1 h, followed by AlexaFluor 488-conjugated goat anti-rabbit IgG, Texas-Red phalloidon (1:200) and DAPI (1:10 000) in 2% BSA-PBS. Images were digitally captured on a Nikon Eclipse TE2000-u microscope coupled to a CCD camera using 200× magnification and processed using Adobe Photoshop.

To assess for association of purified rOmpB with cells, HeLa cells plated at 90% confluency (1×10^5 cells/well) in 24 well plates were incubated for 20 min at 37°C/5% CO_2 with 100 μg ml^{-1} of GST or GST–rOmpB$_{36-1334}$ in serum-free DMEM. Cells were then washed five times with PBS, fixed for 20 min at room temperature with 4% PFA in PBS and processed for immunofluorescence as follows: cell-associated GST or GST-OmpB$_{36-1334}$ were stained using an anti-GST rabbit sera (1:500,